1 **Modeling the hydrology and physiology of *Sphagnum* moss in a**
2 **northern temperate bog**
3

4 Xiaoying Shi[1][*], Daniel M. Ricciuto[1], Peter E. Thornton[1], Xiaofeng Xu[2], Fengming Yuan[1],
5 Richard J. Norby[1], Anthony P. Walker[1], Jeffrey Warren[1], Jiafu Mao[1], Paul J. Hanson[1],
6 Lin Meng[3], David Weston[1], Natalie A. Griffiths[1]

7 [1] Climate Change Science Institute and Environmental Sciences Division, Oak Ridge
8 National Laboratory, Oak Ridge, TN 37831, USA

9 [2]Biology Department San Diego State University, San Diego, CA, 92182-4614, USA
10

11 [3] Department of Geological and Atmospheric Sciences, Iowa State University, Ames, IA,
12 50011
13
14

15 [*] To whom correspondence should be addressed

16 Corresponding author's email: shix@ornl.gov

17   Fax: 865-574-2232

18

19
20
21
22
23
24
25
26
27
28
29
30
31
32
33
34
35
36
37
38
39

40 **Abstract**

41

42   Mosses need to be incorporated into Earth system models to better simulate

43 peatland functional dynamics under changing environment. *Sphagnum* mosses are strong

44 determinants of nutrient, carbon and water cycling in peatland ecosystems. However,

45 most land surface models do not include *Sphagnum* or other mosses as represented plant

46 functional types (PFTs), thereby limiting predictive assessment of peatland responses to

47 environmental change. In this study, we introduce a moss PFT into the land model

48 component (ELM) of the Energy Exascale Earth System Model (E3SM), by developing

49 water content dynamics and non-vascular photosynthetic processes for moss. The model

50 was parameterized and independently evaluated against observations from an

51 ombrotrophic forested bog as part of the Spruce and Peatland Responses Under Changing

52 Environments (SPRUCE) project. Inclusion of a *Sphagnum* PFT with some *Sphagnum*

53 specific processes in ELM allows it to capture the observed seasonal dynamics of

54 *Sphagnum* gross primary production (GPP), albeit with an underestimate of peak GPP.

55 The model simulated a reasonable annual net primary production (NPP) for moss but

56 with less interannual variation than observed, and reproduced above ground biomass for

57 tree PFTs and stem biomass for shrubs. Different species showed highly variable

58 warming responses under both ambient and elevated atmospheric CO_2 concentrations,

59 and elevated CO_2 altered the warming response direction for the peatland ecosystem.

60 Microtopography is critical: *Sphagnum* mosses on hummocks and hollows were

61 simulated to show opposite warming responses (NPP decreasing with warming on

62 hummocks, but increasing in hollows), and hummock *Sphagnum* was modeled to have

63 strong dependence on water table height. Inclusion of this new moss PFT in global ELM

64   simulations may provide a useful foundation for the investigation of northern peatland

65   carbon exchange, enhancing the predictive capacity of carbon dynamics across the

66   regional and global scales.

67   **Copyright statement**

68   This manuscript has been authored by UT-Battelle, LLC under Contract No. DE-

69   AC05-00OR22725 with the U.S. Department of Energy. The United States Government

70   retains and the publisher, by accepting the article for publication, acknowledges that the

71   United States Government retains a non-exclusive, paid-up, irrevocable, world-wide

72   license to publish or reproduce the published form of this manuscript, or allow others to

73   do so, for United States Government purposes. The Department of Energy will provide

74   public access to these results of federally sponsored research in accordance with the DOE

75   Public Access Plan (http://energy.gov/downloads/doe-public-access-plan).

76
77   **1. Introduction**
78
79   Boreal peatlands store at least 500 Pg of soil carbon due to incomplete

80   decomposition of plant litter inputs resulting from a combination of low temperature and

81   water-saturated soils. Because of this capacity to store carbon, boreal peatlands have

82   played a critical role in regulating the global climate since the onset of the Holocene

83   (Frolking and Roulet, 2007; Yu et al., 2010). The total carbon stock is large but

84   uncertain: a new estimation of northern peatlands carbon stock of 1055 Pg was recently

85   reported by Nichols and Peteet (2019). The rapidly changing climate at high latitudes is

86   likely to impact both primary production and decomposition rates in peatlands,

87   contributing to uncertainty in whether peatlands will continue their function as net carbon

88   sinks in the long term (Moore et al., 1998; Turetsky et al., 2002; Wu and Roulet, 2014).

89   Manipulative experiments and process-based models are thus needed to make defensible

90   projections of net carbon balance of northern peatlands under anticipated global warming

91   (Hanson et al, 2017; Shi et al., 2015).

92   Peatlands are characterized by a ground layer of bryophytes, and the raised or

93   ombrotrophic bogs of the boreal zone are generally dominated by *Sphagnum* mosses that

94   contribute significantly to total ecosystem CO_2 flux (Oechel and Van Cleve, 1986;

95   Williams and Flanagan, 1998; Robroek et al., 2009; Vitt, 2014). *Sphagnum* mosses also

96   strongly affect the hydrological and hydrochemical conditions at the raised bog surface

97   (Van, 1995; Van der Schaaf, 2002). As a result, microclimate and *Sphagnum* species

98   interactions influence the variability of both carbon accumulation rates and water

99   exchanges between and within peatlands (Heijmans et al., 2004a, 2004b; Rosenzweig et

100   al., 2008; Brown et al., 2010; Petrone et al., 2011; Goetz and Price, 2015). Functioning as

101   keystone species of boreal peatlands, *Sphagnum* mosses strongly influence the nutrient,

102   carbon and water cycles of peatland ecosystems (Nilsson and Wardle, 2005; Cornelissen

103   et al., 2007; Lindo and Gonzalez, 2010; Turetsky et al., 2010; Turetsky et al., 2012), and

104   exert a substantial impact on ecosystem net carbon balance (Clymo and Hayward; 1982;

105   Gorham, 1991; Wieder, 2006; Weston et el., 2015; Walker et al., 2017; Griffiths et al.,

106   2018).

107   Numerical models are useful tools to identify knowledge gaps, examine long-term

108   dynamics, and predict future changes. Earth system models (ESMs) simulate global

109   processes, including the carbon cycle, and are primarily used to make future climate

110   projections. Poor model representation of carbon processes in peatlands is identified as a

111   deficiency causing biases in simulated soil organic mass and heterotrophic respiratory

112   fluxes for current ESMs (Todd-Brown et al., 2013; Tian et al., 2015). Although most

113   ESMs do not include moss, a number of offline dynamic vegetation models and

114   ecosystem models do include one or more moss plant functional types (PFTs) (Pastor et

115   al., 2002; Nungesser, 2003; Zhuang et al., 2006; Bond-Lamberty et al., 2007; Heijmans et

116   al., 2008; Euskirchen et al., 2009; Wania et al., 2009; Frolking et al., 2010). Several

117   peatland-specific models contain moss species and have been applied globally or at

118   selected peatland sites. For example, the McGill Wetland Model (MWM) was evaluated

119   using the measurements at Degerö Stormyr and the Mer Bleue bogs (St-Hilaire et al.,

120   2010). The peatland version of the General Ecosystem Simulator - Model of Raw Humus,

121   Moder and Mull (GUESS-ROMUL) was used to simulate the changes of daily CO_2

122   exchange rates with water table position at a fen (Yurova et al., 2007). The PEATBOG

123   model was implemented to characterize peatland carbon and nitrogen cycles in the Mer

124   Bleue bog, including moss PFTs but without accounting for microtopography (Wu et al.,

125   2013a). The CLASS-CTEM model (the coupled Canadian Land Surface Scheme and the

126   Canadian Terrestrial Ecosystem Model), which includes a moss layer as the first soil

127   layer, was applied to simulate water, energy and carbon fluxes at eight different peatland

128   sites (Wu et al., 2016). The IAP-RAS (Institute of Applied Physics – Russian Academy

129   of Sciences) wetland methane (CH_4) model with a 10 cm thick moss layer (Mokhov et al.

130   2007) was run globally to simulate the distribution of CH_4 fluxes (Wania et al., 2013).

131   The CHANGE model (a coupled hydrological and biogeochemical process simulator),

132   which includes a moss cover layer (Launiainen et al., 2015), was used to investigate the

133   effect of moss on soil temperature and carbon flux at a tundra site in Northeastern Siberia

134   (Park et al., 2018). Two models, the "ecosys" model (Grant et al., 2012) and

135   CLM_SPRUCE (Shi et al., 2015), have been parameterized to represent peatland

136   microtopographic variability (e.g., the hummock and hollow microterrain characteristic

137   of raised bogs) with lateral connections across the topography. Prediction of water table

138   dynamics in the "ecosys" model is constrained by specifying a regional water table at a

139   fixed height and a fixed distance from the site of interest, thereby missing key controlling

140   factors of a precipitation-driven dynamic water table (Shi et al., 2015). The

141   CLM_SPRUCE model (Shi et al., 2015) was developed to parameterize the hydrological

142   dynamics of lateral transport for microtopography of hummocks and hollows in the raised

143   bog environment of the SPRUCE (Spruce and Peatland Responses Under Changing

144   Environments) experiment (Hanson et al., 2017). That model version did not include the

145   biophysical dynamics of *Sphagnum* moss, and used a prescribed leaf area instead of

146   allowing leaf area to evolve prognostically. In this study, we introduce a new *Sphagnum*

147   moss PFT into the model, and migrate the entire raised-bog capability into the new

148   Energy Exascale Earth System Model (E3SM), specifically into version 1 of the E3SM

149   land model (ELM v1, Ricciuto et al., 2018). The objectives of this study are to: 1)

150   introduce a *Sphagnum* PFT to the ELM model with additional *Sphagnum*-specific

151   processes; and 2) apply the updated ELM to explore how an ombrotrophic, raised-dome

152   bog peatland ecosystem will respond to different scenarios of warming and elevated

153   atmospheric CO_2 concentration.

154   **2. Model description**

155   **2.1 Model provenance**

156   ELM v1 is the land component of E3SM v1, which is supported by the US

157   Department of Energy (DOE). Developed by multiple DOE laboratories, E3SM consists

158   of atmosphere, land, ocean, sea ice, and land ice components, linked through a coupler

159   that facilitates across-component communication (Golaz et al., 2019). ELM was

160   originally branched from the Community Land Model (CLM4.5, Oleson et al., 2013),

161   with new developments that include representation of coupled carbon, nitrogen, and

162   phosphorus controls on soil and vegetation processes, and new plant carbon and nutrient

163   storage pools (Ricciuto et al., 2018; Yang et al., 2019; Burrows et al., in review). The

164   model version used in this study is designated ELM_SPRUCE, and includes the new

165   implementation of *Sphagnum* mosses as well as the hydrological dynamics of lateral

166   transport between hummock and hollow microtopographies. The implementation has

167   been parameterized based on observations from the S1-Bog in northern Minnesota, USA,

168   as described by Shi et al. (2015), with additional details provided below.

169

170   **2.2 New model developments**

171   **2.2.1 Water content dynamics of *Sphagnum* mosses**

172   The main sources for water content of *Sphagnum* mosses are passive capillary

173   water uptake from peat, and interception of atmospheric water on the capitulum (growing

174   tip of the moss) (Robroek et al. 2007). Capillary water uptake, the internal *Sphagnum*

175   moss water content, is modeled as functions of soil water content and evaporation losses.

176   Water intercepted on the *Sphagnum* moss capitulum is modeled as a function of moss

177   foliar biomass, current canopy water, water drip, and evaporation losses.

178   Since evaporation at the *Sphagnum* surface depends on capillary wicking of water

179   up to the surface and atmospheric water vapor deficit, we developed a relationship

180   between measured soil water content at depth, and surface *Sphagnum* water content. At

181   SPRUCE, the peat volumetric water content is measured at several depths using

182   automated sensors (model 10HS, Decagon Devices, Inc., Pullman, WA) calibrated for the

183   site-specific upper peat soil (reference Figure S1, Hanson et al. 2017). We periodically

184   sampled the surface *Sphagnum* for gravimetric water content and water potential using a

185   dew point potentiometer (WP4, Decagon Devices, Inc.). The automated measurements of

186   peat water content at 10 cm depth were shown to be a good indicator of surface

187   *Sphagnum* water content (Fig. 1). Based on this relationship, we model the water content

188   of *Sphagnum* moss due to capillary rise ($W_{internal}$) (g water /g dry moss) as:

189     $W_{internal} = 0.3933 + 7.6227/(1 + \exp(-(Soil_{vol} - 0.1571))/0.018$ (1)

190   where $Soil_{vol}$ is the averaged volumetric soil water of modeled soil layers nearest the

191   10cm depth horizon (layers 3 and 4 in the ELM v1 vertical layering scheme).

192   The *Sphagnum* moss surface water ($W_{surface}$) was calculated using the model

193   predicted canopy water and the dry foliar biomass as:

194 $W_{surface} = can\_water/fmass$ (2)

195   where $W_{surface}$ (g water /g dry moss) is the surface water content and $fmass$ is the foliar

196   biomass of *Sphagnum* mosses. The canopy_water is the *Sphagnum* moss canopy water

197   and it is simulated by a function of interception, canopy drip and canopy evaporation

198   (Oleson et al., 2013).

199   The total water content (W_{total}) of *Sphagnum* mosses is the sum of water taken

200   up from peat and the surface water content (St-Hilaire et al, 2010; Wu et al., 2013).

201     $W_{total} = W_{internal} + W_{surface}$ (3)

202
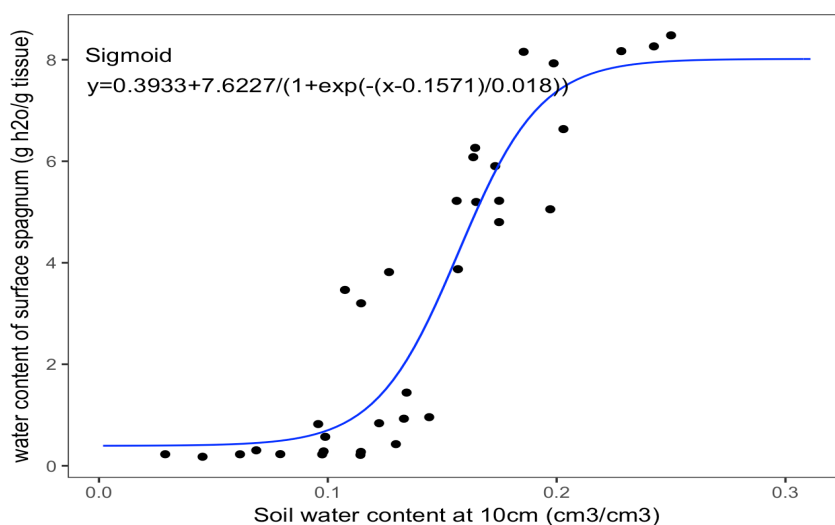
203
204   Figure 1. The measured relationship between soil water content and the water content of surface
205   Sphagnum.
206
207   **2.2.2 Modeling *Sphagnum* CO₂ conductance and photosynthesis**

208   ELM_SPRUCE computes photosynthetic carbon uptake (gross primary

209   production, or GPP) for each vascular PFT on a half-hourly time step, based on the

210   Farquhar biochemical approach (Farquhar et al., 1980; Collatz et al., 1991, 1992), with

211   implementation as described by Oleson et al. (2013). The internal water content of

212   *Sphagnum* mosses is observed to affect photosynthesis by constraining the length of the

213   diffusive path for CO₂ through the variably-hydrated external hyaline cells to the carbon

214   fixation sites (Robroek et al., 2009; Rydin and Jeglum, 2006). Goetz and Price (2015)

215   also indicated that capillary rise through the peat is essential to maintain a water content

216   sufficient for photosynthesis for *Sphagnum* moss species, but that atmospheric inputs can

217   provide small but critical amounts of water for physiological processes. *Sphagnum* lacks

218   a leaf cuticle and stomata that regulate water loss and CO_2 uptake in vascular plants

219   (Titus et al. 1983). The primary transport pathway for CO_2 is through the cells and is

220   analogous to mesophyll conductance in higher plants.

221   The stomatal conductance for vascular plant types in ELM_SPRUCE is derived

222   from the Ball-Berry conductance model (Collatz et al., 1991). That model relates

223   stomatal conductance to net leaf photosynthesis, scaled by the relative humidity and the

224   CO_2 concentration at the leaf surface. The stomatal conductance (g_s) and boundary layer

225   conductance (g_b) are required to obtain the internal leaf CO_2 partial pressure (C_i) of

226   vascular PFTs:

227     $$C_i = C_a - (\frac{1.4 g_s + 1.6 g_b}{g_s \, g_b}) P_{atm} A_n \qquad (4)$$

228   where C_i is the internal leaf CO_2 partial pressure, C_a is the atmospheric CO_2 partial

229   pressure, A_n is leaf net photosynthesis (μ mol CO_2 m^{-2} s^{-1}) P_{atm} is the atmospheric

230   pressure, g_s is the leaf stomatal conductance, g_b is the leaf boundary layer conductance,

231   and values 1.4 and 1.6 are the ratios of the diffusivity of CO_2 to H_2O for stomatal

232   conductance and the leaf boundary layer conductance, respectively.

233   For Sphagnum moss photosynthesis, we followed the method from the McGill

234   Wetland Model (St-Hilaire et al. 2010; Wu et al., 2013), which is based on the effects of

235   *Sphagnum* moss water content on photosynthetic capacity (Tenhunen et al., 1976) and

Biogeosciences
Discussions

236   total conductance of CO_2 (Williams and Flanagan, 1998), and replaces the stomatal

237   conductance representation used for vascular PFTs.

238    $$C_i = C_a - \frac{P_{atm} A_n}{g_{tc}}$$ (5)

239   The total conductance to CO_2 (g_{tc}) was determined from a least-squares regression

240   described by Williams and Flanagan (1998) as:

241    $$g_{tc} = -0.195 + 0.134 W_{total} - 0.0256 W_{total}^2 + 0.0028 W_{total}^3 -$$

242    $$0.0000984 W_{total}^4 + 0.00000168 W_{total}^5$$ (6)

243   where W_{total} is as defined in equation (3). This relationship is only valid up to the

244   maximum water holding capacity of mosses.

245   In addition to the water content, the effects of moss submergence were taken into

246   account in the calculation of moss photosynthesis. Walker et al. (2017) reported

247   significant impacts of submergence on measured *Sphagnum* GPP and modeled the effect

248   by modifying the *Sphagnum* leaf (stem) area index. For simplicity, in ELM_SPRUCE,

249   we calculated such impacts on *Sphagnum* GPP directly as a function of the height of

250   simulated surface water, assuming that GPP from the submerged portion of

251   photosynthetic tissue is negligible. GPP is thus reduced linearly according to the

252   following equation:

253    $GPP_{sub} = GPP_{orig} * (h_{moss} - H_2O_{sfc})$ (7)

254   where GPP_{sub} is the GPP corrected for submergence effects, GPP_{orig} is the original GPP,

255   H_2O_{sfc} is the surface water height, and h_{moss} is the height of the photosynthesizing

256   *Sphagnum* layer above the soil surface, set to 5cm in our simulations. If H_2O_{sfc} is equal to

257   or greater than h_{moss}, GPP is reduced to zero. Because in our simulations surface water is

258   never predicted to occur in the hummocks, in practice this submergence effect only

259   affects the moss GPP in the hollows.

260   **3. Methods**

261   **3.1 Site Description**

262   We focused on a high C, ombrotrophic peatland (the S1-Bog) that has a perched

263   water table with limited groundwater influence (Sebestyen et al. 2011, Griffiths and

264   Sebestyen, 2016). This southern boreal bog is located on the Marcell Experimental

265   Forest, approximately 40 km north of Grand Rapids, Minnesota, USA (47.50283 degrees

266   latitude, -93.48283 degrees longitude) (Sebestyen et al. 2011), and is the site of the

267   SPRUCE climate change experiment (http://mnspruce.ornl.gov; Hanson et al., 2017). The

268   S1-Bog has a raised hummock and sunken hollow microtopography, and it is nearly

269   covered by *Sphagnum* mosses. *S. angustifolium* (C.E.O. Jensen ex Russow) and *S. fallax*

270   (Klinggr.) occupy 68% of the moss layer and exist in both hummocks and hollows. *S.*

271   *magellenicum* (Brid.) occupies ~20% of the moss layer and is primarily limited to the

272   hummocks (Norby et al., 2019). The vascular plant community at the S1-Bog is

273   dominated by the evergreen tree *Picea mariana* (Mill.) B.S.P, the deciduous tree *Larix*

274   *laricina* (Du Roi) K. Koch, and a variety of ericaceous shrubs. Trees are present due to

275   natural regeneration following strip cut harvesting in 1969 and 1974 (Sebestyen et al.,

276   2011). The soil of this peat bog is the Greenwood series, a Typic Haplohemist

277   (https://websoilsurvey.sc.egov.usda.gov), and its average peat depth is 2 to 3 m

278   (Parsekian et al., 2012)

279   Northern Minnesota has a subhumid continental climate with average annual

280   precipitation of 768 mm and annual air temperature of 3.3 °C for the time period from

281   1965 to 2005. Mean annual air temperatures at the bog have increased about 0.4 °C per

282   decade over the last 40 years (Verry et al., 2011).

283   **3.2 Field measurements**

284   Multiple observational pre-treatment data were used in this study. Flux-

285   partitioned GPP of *Sphagnum* mosses was derived from measured hourly *Sphagnum*-peat

286   net ecosystem exchange (NEE) flux (Walker et al., 2017). The GPP – NEE relationship

287   was also evaluated using observed vegetation growth and productivity allometric and

288   biomass data on tree species, stem biomass for shrub species (Hanson et al., 2018a and

289   b), and *Sphagnum* pre-treatment net primary productivity (NPP) (Norby et al., 2019).

290   ELM_SPRUCE was driven by climate data (temperature, precipitation, relative humidity,

291   solar radiation, wind speed, pressure and long wave radiation) from 2011 to 2017

292   measured at the SPRUCE S1-Bog (Hanson et al., 2015a and b). The surface weather

293   station is outside of the enclosures and not impacted by the experimental warming

294   treatments that began in 2015. These data are available at https://mnspruce.ornl.gov/.

295
296   **3.3 Simulation of the SPRUCE experiment**

297   Based on measurements at the SPRUCE site, ELM_SPRUCE includes four

298   PFTs: boreal evergreen needleleaf tree (*Picea)*, boreal deciduous needleleaf tree (*Larix)*,

299   boreal deciduous shrub (representing several shrub species), and the newly introduced

300   *Sphagnum* moss PFT. We used measurements from *Sphagnum* moss collected at a

301   tussock tundra site in Alaska (Hobbie 1996) to set several of the model leaf litter

302   parameters for our simulations (Table 1). The values for other parameters have been

303   optimized based on observations at the SPRUCE site (Table 2 and 3, optimization

304   methods described in section 3.4). We prescribe both hummock and hollow

305   microtopographies to have the same fractional PFT distribution. Consistent with Shi et

306   al. (2015), hummocks and hollows were modeled on separate columns with lateral flow

307   of water between them. All the ELM_SPRUCE simulations were conducted using a

308   prognostic scheme for canopy phenology (Olesen et al., 2013).

309   The SPRUCE experiment at the S1-Bog consists of combined manipulations of

310   temperature (various differentials up to +9 °C above ambient) and atmospheric CO_2

311   concentration (ambient and ambient + 500 ppm) applied in 12 m diameter x 8 m tall

312   enclosures constructed in the S1-Bog. The whole-ecosystem warming began in August

313   2015, elevated CO_2 started from June 2016, and various treatments are envisioned to

314   continue until 2025. Extensive pre-treatment observations at the site began in 2009.

315   For the ELM_SPRUCE, we continuously cycled the 2011-2017 climate forcing

316   (see section 3.2) to equilibrate carbon and nitrogen pools under pre-industrial

317   atmospheric CO_2 concentrations and nitrogen deposition, and then launched a simulation

318   starting from year 1850 through year 2017. This transient simulation includes historically

319   varying CO_2 concentrations, nitrogen deposition, and the land-use effects of a strip cut

320   and harvest at the site in 1974. These simulations were used to compare model

321   performance with pre-treatment observations. A subset of these observations was also

322   used for optimization and calibration (section 3.4).

323   To investigate how the bog vegetation may respond to different warming

324   scenarios and elevated atmospheric CO_2 concentrations, we performed 11 model runs

325   from the same starting point in year 2015. These simulations were designed to reflect the

326   warming treatments and CO_2 concentrations being implemented in the SPRUCE

327   experiment enclosures. The model simulations include one ambient case (both ambient

328   temperature and CO_2 concentration), and five simulations with modified input air

329   temperatures to represent the whole-ecosystem warming treatments at five levels (+0 °C,

330   +2.25 °C, +4.50 °C, +6.75 °C and +9.00 °C above ambient) and at ambient CO_2, and

331   another five simulations with the same increasing temperature levels and at elevated CO_2

332   (900 ppm). In the treatment simulations, we also considered the passive enclosure

333   effects, which reduce incoming shortwave and increase incoming longwave radiation

334   (Hanson et al., 2017). Following the SPRUCE experimental design, there was no water

335   vapor added so that the simulations used constant specific humidity instead of constant

336   relative humidity across the warming levels. All the treatment simulations were

337   performed through the year 2025 by continuing to cycle the 2011-2017 meteorological

338   inputs (with modified temperature and radiation to reflect the treatments) to simulate

339   future years.

340   Table 1: Physiological parameters of *Sphagnum* mosses as given in Hobbie 1996

Parameters	Description	Values
lflitcn	Leaf litter C:N ratio (gC/gN)	66
lf_fcel	Leaf litter fraction of cellulose	0.737
lf_flab	Leaf litter fraction of labile	0.227
lf_flig	Leaf litter fraction of lignin	0.036

341

Biogeosciences
Discussions

3.4. Model sensitivity analysis and calibration

The vegetation physiology parameters in ELM_SPRUCE were originally derived

from CLM4.5 and its predecessor, Biome-BGC, and represent broad aggregations of

plant traits over many species and varied environmental conditions (White et al., 2000).

To achieve reasonable model performance at SPRUCE, site-specific parameters and

targeted parameter calibration are needed. Since the ELM_SPRUCE contains over 100

uncertain parameters, parameter optimization is not computationally feasible without first

performing some dimensionality reduction. Based on previous ELM sensitivity analyses

(e.g., Lu et al., 2018; Ricciuto et al., 2018; Griffiths et al., 2018), we chose 35 model

parameters for further calibration (Tables 2 and 3). An ensemble of 3000 ELM_SPRUCE

simulations were conducted using the procedure described in 3.3, with each ensemble

member using a randomly selected set of parameter values within uniform prior ranges.

This model ensemble was first used to construct a polynomial chaos surrogate model,

which was then used to perform a global sensitivity analysis (Sargsyan et al., 2014;

Ricciuto et al., 2018). Main sensitivity indices, reflecting the proportion of output

variance that occurs for each parameter, are described in section 4.1.

To minimize potential biases in model predictions of treatment responses, we

calibrated the same 35 model parameters using pre-treatment observations as data

constraints. We employed a quantum particle swarm optimization (QPSO) algorithm (Lu

et al., 2018). While this method does not allow for the calculation of posterior prediction

uncertainties, it is much more computationally efficient than other methods such as

Markov Chain Monte Carlo. The constraining data included tree growth and biomass

(Hanson et al. 2018a), shrub growth and biomass (Hanson et al., 2018b), *Sphagnum* net

365   primary productivity (Norby et al., 2017, 2019), enclosure-averaged leaf area index by

366   PFT, and water table depth (WTD) observations, aggregated to seasonal averages

367   (Hanson et al., 2015b). The goal of the optimization is to minimize a cost function, which

368   we define here as a sum of squared errors over all observation types weighted by

369   observation uncertainties. When observation uncertainties were not available, we

370   assumed a range of ±25% from the default value. Site measurements were also used to

371   constrain the ranges of two parameters: *leafcn* (leaf carbon to nitrogen ratio) and *slatop*

372   (specific leaf area at canopy top). The uniform prior ranges for these parameters represent

373   the range of plot to plot variability. Optimized parameter values are shown in Table 2 and

374   3. Section 4 reports the results of simulations using these optimized parameters, which

375   were used to perform a spinup, transient (1850-2017) and set of 11 treatment simulations

376   (2015-2025) as described above.

377   Table 2: PFT-specific optimized model parameters

Parameter	Description	*Sphagnum*	*Picea*	*Larix*	Shrub	Range
flnr	Rubisco-N fraction of leaf N	0.2906	0.0678	0.2349	0.2123	[0.05,0.30]
croot_stem	Coarse root to stem allocation ratio	N/A	0.2540	0.1529	0.7540	[0.05,0.8]
stem_leaf[1]	Stem to leaf allocation ratio	N/A	1.047	1.016	0.754	[0.3,2.2]
leaf_long	Leaf longevity (yr)	0.9744	5[3]	N/A	N/A	[0.75, 2.0]
slatop	Specific leaf area at canopy top ($m^2\ gC^{-1}$)	0.00781	0.00462	0.0128	0.0126	[0.004,0.04]
leafcn	Leaf C to N ratio	35.56	70.17	64.84	33.14	[20,75]
froot_leaf[2]	Fine root to leaf allocation ratio	0.3944	0.8567	0.3211	0.6862	[0.15, 2.0]
mp	Ball-Berry stomatal conductance slope	N/A	7.50	9.32	10.8	[4.5, 12]

378   Optimized values of PFT-specific parameters. The range column values in brackets indicate the range of
379   acceptable parameter values used in the sensitivity analysis and the optimization across all four PFTs in the
380   format [minimum, maximum]. N/A indicates that parameter is not relevant for that PFT.

381 [1]for tree PFTs, this parameter depends on NPP. The value shown is the allocation at an NPP of 800 gC m^{-2}
382 yr^{-1}.
383 [2] the fine root pool is used as a surrogate for non-photosynthetic tissue in *Sphagnum*
384 [3] This parameter was not optimized; we used the default value.
385
386
387

388

389 Table 3: Non PFT-specific optimized model parameters

	Description	Optimized value	Default	Range
r_mort	Vegetation mortality	0.0497	0.02	[0.005, 0.1]
decomp_depth_efolding	Depth-dependence e-folding depth for decomposition (m)	0.3899	0.5	[0.2, 0.7]
$q_{drai,0}$	Maximum subsurface drainage rate (kg m^{-2} s^{-1})	3.896e-6	9.2e-6*	[0, 1e-3]
Q_{10}_mr	Temperature sensitivity of maintenance respiration	2.212	1.5	[1.2, 3.0]
br_mr	Base rate for maintenance respiration (gC gN m^2 s^{-1})	4.110e-6	2.52e-6	[1e-6, 5e-6]
crit_onset_gdd	Critical growing degree days for leaf onset	99.43	200	[20, 500]
lw_top_ann	Live wood turnover proportion (yr^{-1})	0.3517	0.7	[0.2, 0.85]
gr_perc	Growth respiration fraction	0.1652	0.3	[0.12, 0.4]
$r_{drai,0}$	Coefficient for surface water runoff (kg m^{-4} s^{-1})	6.978e-7	8.4e-8*	[1e-9, 1e-6]

390 Optimized and default values for non PFT-specific parameters. The range column values in brackets
391 indicate the range of acceptable parameter values used in the sensitivity analysis and the
392 optimization in the format [minimum, maximum].
393 • Previously calibrated value from Shi et al (2015)

394

395 **4. Results**

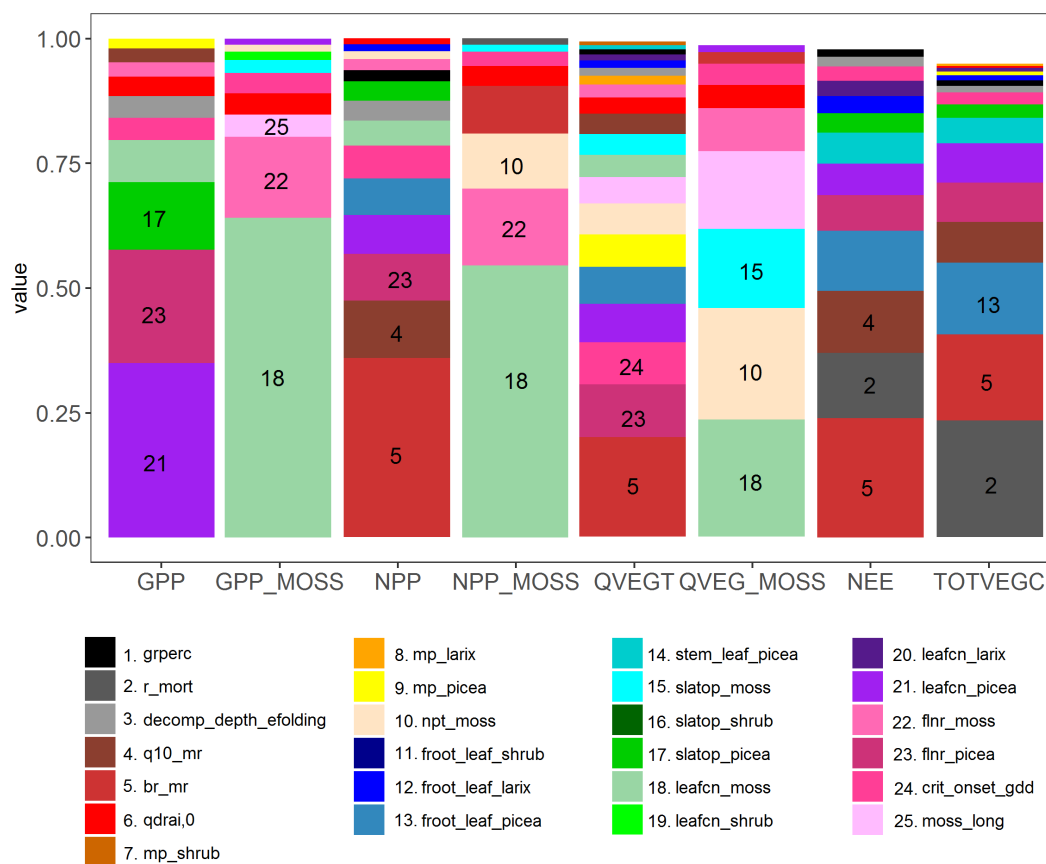396 **4.1 Model sensitivity analysis**

397   Main effect (first-order) sensitivities are shown for eight model output quantities of

398   interest: Total site gross primary productivity (GPP), GPP for the moss PFT only

399   (GPP_moss), total site net primary productivity (NPP), NPP for the moss PFT only

400   (NPP_moss), total site vegetation transpiration (QVEGT), evaporation from the moss

401   surface (QVEG_moss), net ecosystem exchange (NEE) and site total vegetation carbon

402   (TOTVEGC) (Fig. 2). Out of 35 parameters investigated, 25 show a sensitivity index of

403   at least 0.01 for one of the quantities of interest, and these are plotted on figure 2. In that

404   figure, sensitivities are stacked in order from highest to lowest for each variable, with the

405   height of the bar equal to the sensitivity index. The first order sensitivities sum to at least

406   0.95 for all variables, indicating that higher order sensitivities (i.e., contributions to the

407   sensitivity from combinations of two or more parameters) contribute relatively little to

408   the variance for these quantities of interest.

409   According to this analysis, the variance in total site GPP is dominated by three

410   *Picea* parameters: the fraction of leaf nitrogen in RuBiCO (*flnr_picea)*, leaf carbon to

411   nitrogen ratio (*leafcn_picea)* and the specific leaf area at canopy top (*slatop_picea*). GPP

412   sensitivity for the moss PFT is dominated by the same three parameters, but for the moss

413   PFT instead of *Picea* (*flnr_moss*, *leafcn_moss*, and *slatop_moss*). For NPP, QVEGT and

414   NEE, the highest sensitivity the maintenance respiration base rate *br_mr*, similar to

415   earlier results in Griffiths et al. (2017). The maintenance respiration temperature

416   sensitivity Q_{10}_mr is also a key parameter for NPP and NEE. The critical onset growing

417   degree day threshold (*crit_onset_gdd*), which drives deciduous phenology in the spring

418   for the *Larix* and shrub PFTs, is an important parameter for NPP and NEE. *flnr_picea* is

419   important for both NPP and QVEGT. For NPP_moss and QVEG_moss, *leafcn_moss* is

420   and the ratio of non-photosynthesizing tissue to photosynthesizing tissue (*npt_moss*) are

421   sensitive. For TOTVEGC and NEE, vegetation mortality (*r_mort*) is also a sensitive

422   parameter. For the site-level quantities of interest, at least 10 parameters contribute

423   significantly to the uncertainty, illustrating the complexity of the model and large number

424   of processes contributing to uncertainty in SPRUCE predictions. For the moss variables,

425   there are some cases where significant sensitivities exist for non-moss PFT parameters.

426   For example, *leafcn_shrub* is the seventh most sensitive parameter for GPP_moss,

427   indicating that competition between the PFTs for resources may be important. In this

428   case, uncertainty about parameters on one PFT may drive uncertainties in the simulated

429   productivity of other PFTs.

Biogeosciences
Discussions

Figure 2 Sensitivity analysis of ELM-SPRUCE for selected parameters (Table 2 and 3). The Colored bars indicate the fraction of variance in site gross primary productivity (GPP), moss-only NPP (GPP_MOSS), site net primary productivity (NPP), moss-only NPP (NPP_MOSS), total vegetation transpiration (QVEGT), moss evaporation (QVEG_MOSS), site net ecosystem exchange (NEE) and total vegetation carbon (TOTVEGC) controlled by each parameter. The legend shows the top 25 most influential parameters; the remaining parameters not shown have sensitivities of no more than 0.01 for any of the outputs. All variables represent 2011-2017 average values over the ambient conditions. For parameters that are treated as PFT-dependent, the PFT is indicated with a suffix (picea, larix, shrub or moss)

4.2 Model evaluation

Our model simulates GPP for vascular plants and *Sphagnum* moss in both

hummock and hollow settings, with separate calculations for each PFT. Here we use the

444   model estimate of GPP prior to downregulation by nutrient limitation from the ambient

445   case, based on recent studies indicating that nutrient limitation effects are occurring

446   downstream of GPP (Raczka et al. 2016; Metcalfe et al., 2017; Duarte et al. 2017). This

447   treatment of nutrient limitation on GPP has been modified in a more recent version of

448   ELM, and our moss modifications will be merged to that version as a next step. For now,

449   by referring to the pre-downregulation GPP we are capturing the most significant impact

450   of those changes for the purpose of comparison to observations.

451   Our model simulated two seasonal maxima of *Sphagnum* moss GPP, one at the

452   end of May, and the other in August (Figure 3). Both peaks are lower than the maximum

453   of observed (flux-partitioned) GPP, which occurs in August. Based on results of the

454   sensitivity analysis, it could be that the base rate for maintenance respiration for moss is

455   too high, causing an underestimate of NPP and biomass, which leads to a low bias in

456   peak GPP.

457   During June and October, observations suggest that ELM_SPRUCE over-predicts

458   GPP. The model does limit GPP as a function of the depth of standing water on the bog

459   surface (Eq. 7). The water table height (WTH) above the bog surface is being predicted

460   by the model (dashed red line in Fig. 3), and while the seasonal pattern of higher water

461   table in the spring and lower water table in the fall agrees well with observations (dashed

462   black line in Fig. 3), the predicted WTH is generally too low by 5-10 cm. The modeled

463   WTH here is for hollow. We turned off the lateral transport when there is ice on the soil

464   layers above the water table to avoid an unreasonable amount of ice accumulation on the

465   frozen layers, which results in there is no flow from hummock to hollow. Forcing the

466   modeled GPP to respond to observed WTH (during the period with observations) gives a

467   pattern of increasing GPP through June and July which is more consistent with

468   observations (blue line in Fig. 3). We do not have observations for GPP earlier than June,

469   due to limitations of the instrumentation when the bog surface is flooded.
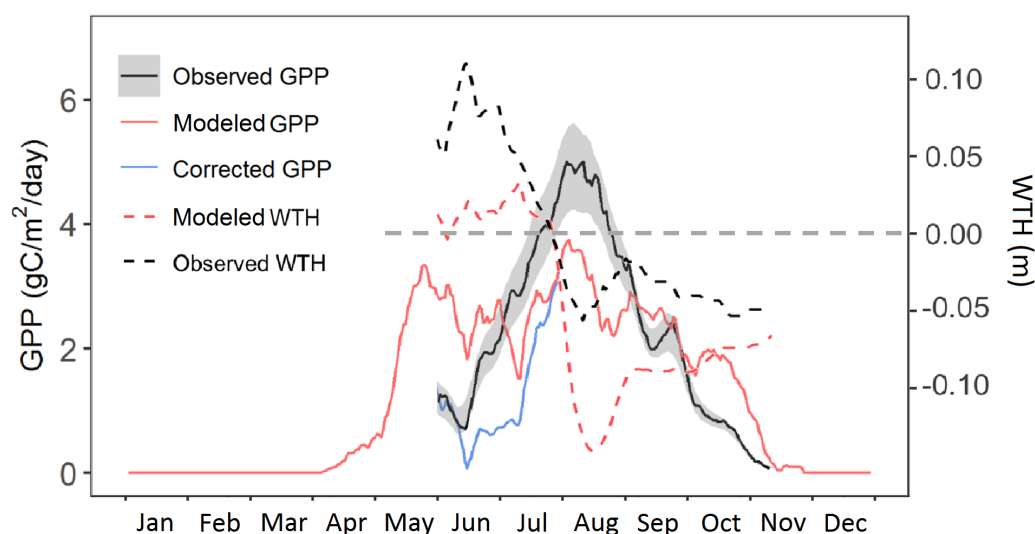

470
471
472   Figure 3. Predicted GPP (red solid line) compared with flux-partitioned GPP (black solid line) of
473   *Sphagnum* mosses for the year 2014. The blue line is the predicted GPP corrected with the
474   observed water table height. The dashed black and red lines are observed and modeled water table
475   height (the dashed gray line is the hollow surface).
476
477
478   The model simulated reasonable annual values for *Sphagnum* NPP for the period

479   2014-2017 but showed much lower NPP compared with observation (139 vs. 288 g

480   C/m^2/yr) for the year 2012 (Fig. 4a). Measurement uncertainties are larger in 2016-2017

481   than in earlier years, perhaps related to a new measurement protocol for those years, and

482   the model estimates are within measurement uncertainty bounds for years 2014-2017

483   (Griffiths et al., 2018; Norby et al., 2019). The observed *Sphagnum* NPP was measured at

484   different plots and each plot included different species abundances. As a result, the scaled

485   NPP includes spatial variations and uncertainty in species distribution (Norby and Childs,

486   2017).

487   Simulated tree above ground biomass is within the observed inter-plot variability

488   (Fig. 4b). Observations suggest an increasing trend in tree biomass, which was not

489   predicted by the model. The optimized parameters show increased mortality and

490   autotrophic respiration rate parameters compared to the default model (Table 3), which

491   causes the simulations to approach steady state relatively quickly after the 1974

492   disturbance. However, the sensitivity analysis also identifies theses mortality and

493   maintenance respiration parameters as highly sensitive, therefore this simulated response

494   is uncertain. For the shrub stem carbon, the simulated mean from year 2012 to 2015 was

495   140.4 g C/m^2, slightly higher than the observation (133.9 g C/m^2) but well within the

496   observed range of inter-plot variability (Fig. 4c).
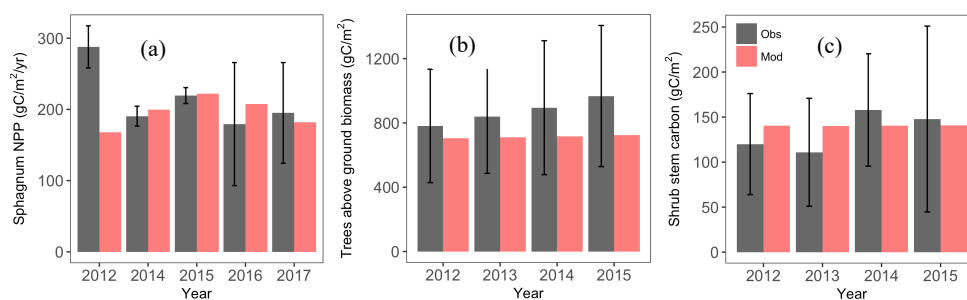
497

498   Figure 4. Predicted (red bars) *Sphagnum* NPP (left), aboveground tree biomass (middle) and
499   shrub stem carbon (right) compared with the observations (black bars). Observed NPP data are
500   based on growth of 12-17 bundles of 10 Sphagnum stems in 2012-2015 (unpublished data) and
501   in two ambient plots by the method described by Norby et al. (2019) in 2016-1017 (data in
502   Norby et al. 2017).
503
504   **4.3 Simulated carbon cycle response to warming and elevated atmospheric CO$_2$**

505   **concentration**

506   Different PFTs demonstrated different warming responses for both ambient CO_2

507   and elevated CO_2 concentration conditions (Fig. 5). Both *Larix* and shrub NPP increased

508   with warming under both CO_2 concentration conditions (Fig. 5 b, c, h and i). In addition,

509   CO_2 fertilization stimulates the growth of these two PFTs and the fertilization effect

510   further increases with warming (Fig. S1, GPP increases more under elevated CO_2

511   condition than the ambient case). In contrast, *Picea* NPP decreased with warming levels

512   (Fig. 5 a and g) for both CO_2 conditions. For *Sphagnum,* NPP decreased in hummocks

513   but increased in hollows with increasing temperature (Fig. 5 d, e, j and k). The enclosure-

514   total NPP for all PFTs responded differently to the warming only and warming with

515   elevated CO_2 (Fig. 5 f and l). The enclosure-total NPP for each warming level changed

516   less under the ambient CO_2 condition than those with elevated CO_2 condition, and NPP

517   decreased with warming in most of years under ambient CO_2 condition but increased

518   under elevated CO_2 condition (Fig.5 f and l). This result demonstrated that the elevated

519   CO_2 scenario changes the sign of the NPP warming response for the bog peatland

520   ecosystem.
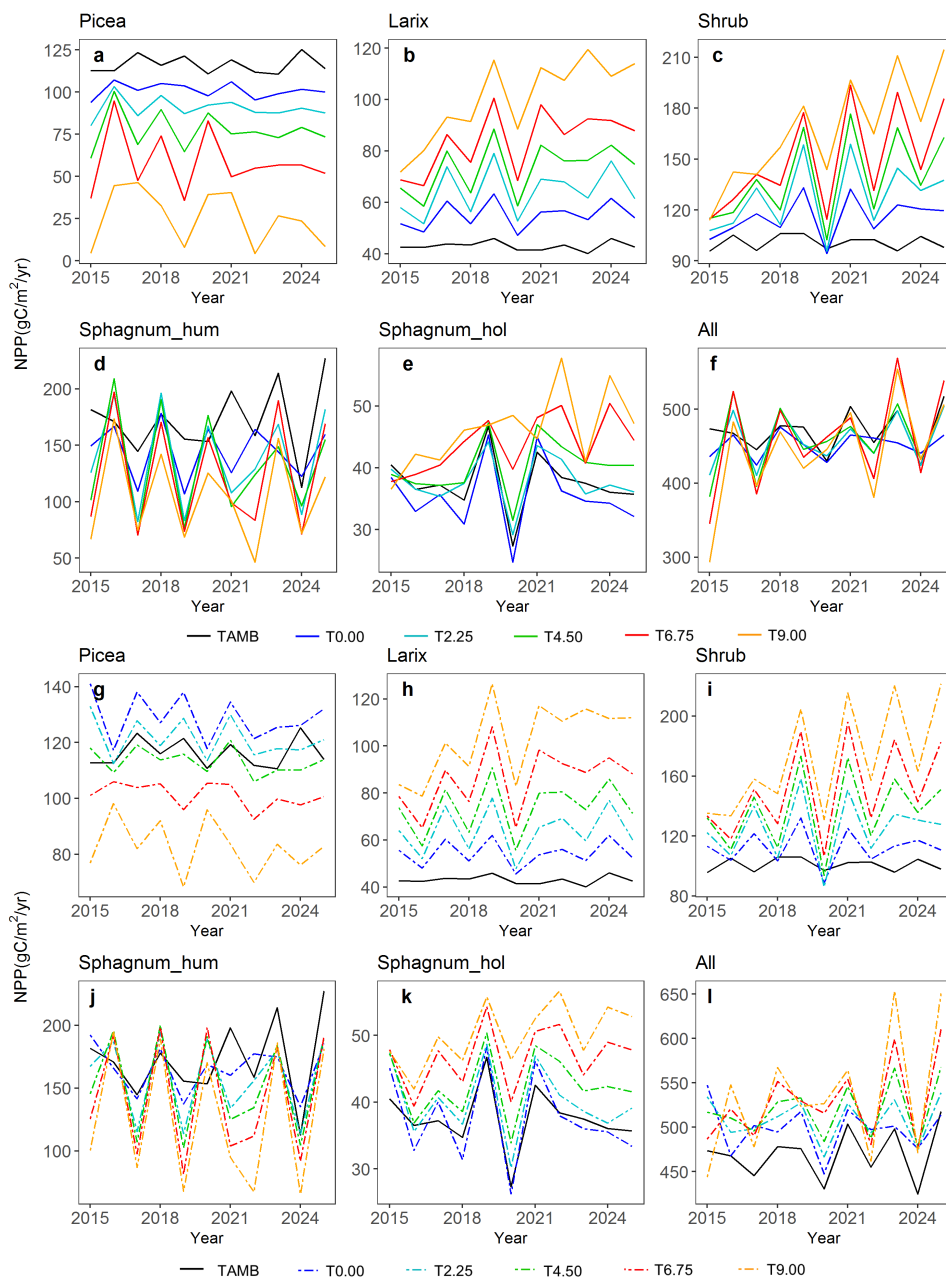
521
522 Figure 5 predicted NPP response to warming with ambient atmospheric CO_2 (a-f, solid lines) and
523 warming with elevated atmospheric CO_2 concentration (g-l, dash lines), the black solid line
524 TAMB is the ambient temperature and CO_2 case, T0.00 to T9.00 means increasing temperature
525 from 0°C to 9°C
526

527   Compared with the ambient biomass, the biomass of black spruce (*Picea*)

528   significantly decreased but the biomass of *Larix* significantly increased under the greatest

529   warming treatment (+9.00℃, Fig.6). Biomass of shrub and hollow *Sphagnum* also

530   increased, but less than did *Larix*. The hummock *Sphagnum* biomass also showed strong

531   correlation with water table height at roughly a 3-month lag (the maximum correlation

532   occurs with an 82-day lag, R^2=0.56). Due to the relative lower height of the water table in

533   the hummock than the hollow, the simulated hummock *Sphagnum* were more

534   significantly water-stressed than the hollow *Sphagnum* as the water table height declines.

535   This is consistent with multiple studies finding an increase in temperatures associated

536   with drought (low water table height) reducing *Sphagnum* growth (Bragazza et al., 2016;

537   Granath et al., 2016; Mazziotta et al., 2018). In summary, the growth of bog vegetation is

538   predicted to have species-specific warming responses that differ in sign and magnitude.
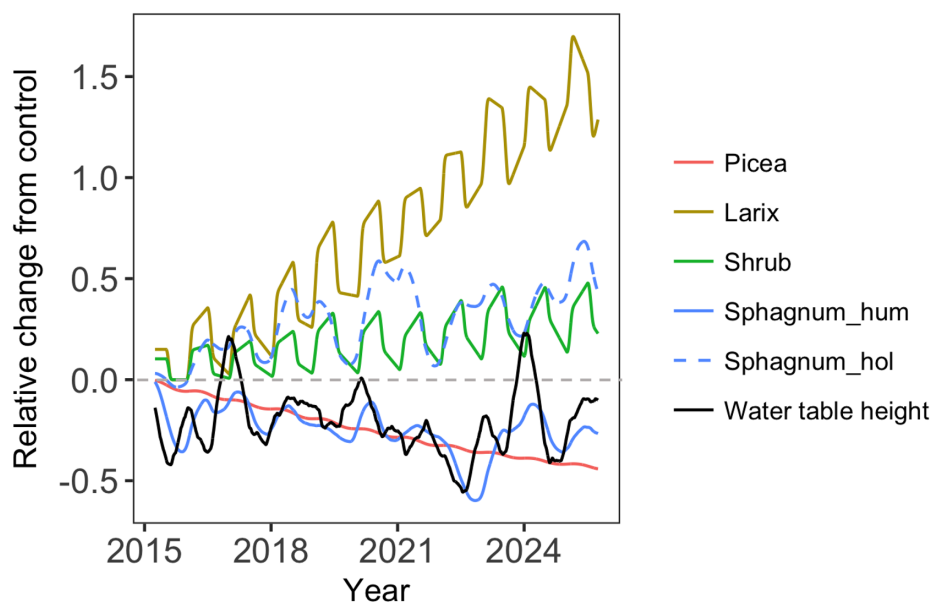
539
540   Figure 6 The relative changes of biomass for different PFTs and water table height (the weighted
541   average between hummock and hollow) between +9.00 ℃ treatment case and the ambient case
542   (+9.00 ℃ / ambient – 1)

543   **5. Discussion**
544
545   Sphagnum moss is the principal plant involved in the peat accumulation in peatland

546   ecosystems, and effective characterization of its biophysical and physiological responses

547   has implications for predicting peatland and global carbon, water and climate feedbacks.

548   This study moves us closer to our long-term goal of improving the prediction of peatland

549   water and carbon cycles in ELM, by introducing a new *Sphagnum* moss PFT,

550   implementing water content dynamics and photosynthetic processes for this nonvascular

551   plant. The *Sphagnum* model development combined with our previous hummock-hollow

552   microtopography representation and laterally-coupled two-column hydrology scheme

553   enhance the capability of ELM_SPRUCE in simulating high-carbon wetland hydrology

554   and carbon interactions and their responses to plausible environmental changes.

555
556   **5.1 Uncertainties in simulating *Sphagnum* productivity**

557   Our predicted peak GPP is similar to the results found by Walker et al. (2017)

558   when they calculated the internal resistance to CO_2 diffusion as a function of *Sphagnum*

559   water content using a stand-alone photosynthesis model. In both cases, the predicted peak

560   GPP is lower than observations. Walker et al. (2017) were, however, able to capture the

561   observed peak magnitude with a combination of light extinction coefficient, canopy

562   clumping coefficient, maximum shoot area index (SAI), and a logistic function

563   describing the effective *Sphagnum* SAI in relation to water table. Here we used model

564   default values for the light extinction and canopy clumping coefficients. While the water

565   table impacts *Sphagnum* productivity in our simulation, modeled leaf (or shoot) area

566   index (LAI) is mainly controlled by NPP and turnover. Further investigation is thus

567   needed to understand how representative the chamber-based observations from Walker et

568   al. (2017) are of the larger-scale SPRUCE enclosures, and to reconcile these GPP

569   estimates with plot-level NPP observations (Norby et al., 2019).

570   The water table depth (WTD) is also a key factor that influences the seasonality of

571   GPP in *Sphagnum* mosses (Lafleur et al., 2005; Riutta 2007, Sonnentag et al, 2010; Grant

572   et al., 2012; Kuiper et al., 2014; Walker et al, 2017). Previous studies have reported that

573   drier and warmer future climates can lower the water table, affecting the resilience of

574   long-term boreal peatland carbon stocks (Limpens et al., 2008, Dise, 2009, Frolking et

575   al., 2011). WTD drawdown affects the net ecosystem productivity of boreal peatlands

576   through its effects on ecosystem respiration and GPP. The interactions between WTD and

577   GPP, however, vary across peatlands and influence both vascular and nonvascular plant

578   GPP in different ways (Lafleur et al., 2005). For instance, nonvascular plants mostly

579   access water in the near surface shallow peat layers. These layers, however, can drain

580   quickly with receding WTD and high nonvascular evaporative demand, and thus depend

581   on water supply through capillary rise or precipitation (Dimitrov et al., 2011, Peichl et al.,

582   2014). If recharge is not adequate, near-surface peat desiccation occurs thereby cutting

583   off the supply of water to *Sphagnum*, which subsequently dries, leading to rapid decline

584   in GPP (Lafleur et al., 2005, Riutta 2008, Sonnentag et al ., 2010, Sulman et al., 2010,

585   Dmitrov et al., 2011, Kuiper et al., 2014, Peichl et al., 2014). Alternately, under saturated

586   conditions when the water table is close to the *Sphagnum* surface, *Sphagnum*

587   photosynthesizing tissue can become submerged or surrounded by a film of water that is

588   likely to reduce the effective LAI of the *Sphagnum* and thus reduce photosynthesis

589   (Walker et al., 2017). One study reported that submerged Sphagnum can take up carbon

590   derived from CH4 via symbiotic methanatrophs (Raghoebarsing et al., 2005), but in any

591   cases CO_2 diffusion for photosynthesis will dramatically decrease under water.

5.2 Predicted warming response uncertainties
592

593

594   Our model warming simulations suggested that increasing temperature reduced

595   the *Picea* growth but increased the growth of *Larix* under both ambient and elevated

596   atmospheric CO_2 conditions. The main reason for this model difference in response for

597   the two tree species is that despite their similar productivity under ambient conditions,

598   *Picea* has more respiring leaf and fine root biomass because of lower specific leaf area,

599   longer leaf longevity, and higher fine root allocation. Therefore, warming results in a

600   much larger increase in maintenance respiration relative to changes in NPP for *Picea*

601   compared to *Larix* (Fig. 5 and Fig. S2). Increased tree growth and productivity in

602   response to the recent climate warming for high-latitude forests has been reported

603   (Myneni et al., 1997, Chen et al. 1999, Wilming et al. 2004, Chavardes, 2013). On the

604   other hand, reductions in tree growth and negative correlations between growth and

605   temperature also have been shown (Barber et al., 2000; Wilmking et al., 2004; Silva et

606   al., 2010; Juday and Alix 2012; Girardin et al., 2016; Wolken et at., 2016).

607   Our model also predicted increasing growth of shrubs with increased temperature,

608   similar to simulated increase in shrub cover caused mainly by warmer temperatures and

609   longer growing seasons reported by Miller and Smith (2012) using their model LPJ-

610   GUESS. In addition, several other modelling studies have also found increased biomass

611   production and LAI related to shrub invasion and replacement of low shrubs by taller

612   shrubs and trees in response to increased temperatures in tundra regions (Zhang et al.,

613   2013; Miller and Smith, 2012; Wolf et al., 2008; Rydssa et al., 2017).

614   The responses of *Sphagnum* mosses to warming simulated by ELM_SPRUCE

615   showed that *Sphagnum* growth in hollows was consistently higher with increased

616   temperatures, where water availability was not limiting. *Sphagnum* growing on

617   hummocks, on the other hand, showed negative warming responses and strong

618   dependency on water table height. Previous studies have shown that moss growth may be

619   reduced directly by higher air temperature, due to the relatively low temperature optima

620   of moss photosynthesis (Hobbie et al.,1999), and can be reduced by water stress (Norby

621   et al., 2019). Moreover, increased shading by the shrub canopy and associated leaf litter

622   could indirectly decrease moss growth (Chapin et al., 1995; Hobbie and Chapin 1998;

623   Van der Wal et al., 2005; Walker et al., 2006; Breeuwer et al., 2008. Other studies

624   suggest that Sphagnum growth can be promoted via a cooling effect of shading on the

625   peat surface, by alleviating photo-inhibition of photosynthesis and also by reducing

626   evaporation stress (Busby et al., 1978; Murray et al., 1993; Man et al., 2008; Walker et

627   al., 2015, Bragazza et al., 2016, Mazziotta et al., 2018). Currently ELM_SPRUCE does

628   not include light competition among multiple PFTs, and thus does not represent cross-

629   PFT shading effects. ELM_SPRUCE does predict enhancement of shrub and *Larix* tree

630   with increased temperatures with both ambient and elevated CO_2 conditions (the leaf area

631   increasing with warming, Fig. S3). Norby et al. (2019) showed that the fractional cover

632   of different Sphagnum species declined with warming, but while ELM_SPRUCE allows

633   the canopy density of PFTs to change prognostically, their fractional cover is held

634   constant.

635   It is also encouraging that while we did not use leaf-level gas exchange

636   observations in our optimization, the increased maintenance respiration base rate and

637   temperature sensitivity compared to default (table 2) is largely consistent with pre-

638   treatment leaf level observations (Jensen et al., 2019). In the future, a multi-scale

639   optimization framework that can assimilate leaf and plot-level observations

640   simultaneously should lead to improved model predictions and reduced uncertainties for

641   the treatment simulations. If similar patterns observed in ambient conditions continue

642   during the treatments, incorporating seasonal variations in leaf photosynthetic parameters

643   may also further improve the simulated response to warming (Jensen et al., 2019).

644   Overall, while the sensitivity analysis is useful to indicate the key parameters and

645   mechanisms responsible for uncertainty, our ability to quantify prediction uncertainty is

646   limited because we consider only a single simulation with optimized parameters. Ideally,

647   we should perform a model ensemble that represents the full range of posterior

648   uncertainty over simulations that are consistent with the pre-treatment observations, and

649   also a range of possible future meteorological conditions. This is currently being done for

650   SPRUCE with the TECO carbon cycle model (Jiang et al., 2018), but the computational

651   expense of ELM_SPRUCE currently prohibits this approach. By combining new

652   surrogate modeling approaches (e.g. Lu et al., 2019) with MCMC techniques, it may be

653   possible to achieve this in the near future. This will help to reduce prediction

654   uncertainties, which currently prevail in the future carbon budget of peatlands and its

655   feedback to climate change (McGuire et al., 2009).

656   **5.3 Outstanding issues and future directions**

657   The present modeling framework works well for hydrological dynamics (Shi et

658   al., 2015), vegetation responses (this study), and reconstructing CH_4 dynamics (Ricciuto

659   et al., in review) within the S1-Bog in Minnesota. It will thus be migrated into the E3SM.

660   However, more developments of ELM_SPRUCE are still needed before widespread

661   applications.

662   The live green moss layer buffers the exchange of energy and water at soil surface

663   and regulates the soil temperature and moisture because of its high-water holding

664   capacity and the insulating effect (McFadden et al., 2003; Block et al., 2011; Turesky et

665   al, 2012; Park et al., 2018). Nevertheless, we currently include only one *Sphagnum* moss

666   PFT, and will eventually treat the *Sphagnum* mosses as the "top" soil layer with a lower

667   thermal conductivity and higher hydraulic capacity than a mineral soil layer (Wu et al.,

668   2016). We also intend to model light competition, the shading effect of shrub expansion,

669   and the changes of Sphagnum community composition. Moreover, the new

670   implementation would allow for the simulation of the moss layer acting as a barrier for

671   the water and energy exchange from the underlying organic soil layer with the

672   atmosphere. In addition, we also plan to investigate the ecosystem consequences of loss

673   of Sphagnum from this ecosystem.

674   The current model version is not able to simulate the biogeophysical changes that

675   occur due to the long-term accumulation of peat in the bog; however, previous literature

676   reported that there is a need to develop relatively realistic peatland growth models where

677   the rates of ecosystem processes are a function of climate and the inherent autogenic

678   properties of peatlands (Frolking et al., 2010, Belyea and Baird, 2006; Dies, 2009). Thus,

679   future work requires modeling the peat accumulation and associated feedbacks among

680   hydrology, vegetation communities, and peat properties. This would also facilitate the

681   simulation of basic patterns of peat accumulation over millennia in northern peatlands,

682   including accumulation rates, vegetation and fen-bog transitions, and future impacts from

683   the potential loss of peat under warming scenarios.

684   Nitrogen (N_2) fixation is a major source of available N in ecosystems that receive

685   low amounts of atmospheric N deposition, like boreal forests and subarctic tundra (Lindo

686   et al., 2013, Weston et al, 2015, Rousk et al., 2016, Kostka et al., 2016). For example,

687   diazotrophs are estimated to supply 40-60% of N input to peatlands (Vile et at., 2014)

688   with high accumulation of fixed N into plant biomass (Berg et al., 2013). Nevertheless,

689   N_2 fixation is an energy costly process and is inhibited when N availability and reactive

690   nitrogen deposition is high (Gundale et al., 2011; Ackermann et al., 2012; Rousk et al.,

691   2013). This could limit ecosystem N input via the N_2 fixation pathway. A recent study

692   showed that N_2 fixation activity in the S1-bog was negatively correlated with temperature

693   (Carrell at al., 2019). However, for the current ELM_SPRUCE, N_2 fixation process is

694   only tied to the whole-ecosystem NPP for all PFTs and is not mechanistic. We will focus

695   on this process in future model development.

696   In addition to the simulations aimed at improved understanding of bog response to

697   experimental manipulations at the plot-scale, we are pursuing model implementations at

698   larger spatial scales. The model framework described in this study is capable of

699   performing regional simulations, although the current simulations were designed for

700   mechanistic understanding of *Sphagnum* mosses hydrological and physiological

701   dynamics at the plot-level. We are already exploring the use of high-resolution gridded

702   domains with explicit vertical and lateral flows as a foundation for more highly

703   parameterized simulations that could allow us to estimate water, energy, and greenhouse

704   gas fluxes for large landscapes in which peatland bogs are an important component.

705 **6. Summary**

706   In this study, we reported the development of a *Sphagnum* moss PFT and

707 associated processes within the ELM_SPRUCE model. Before being used to examine the

708 ecosystem response to warming and elevated CO_2 at a temperate bog ecosystem, the

709 updated model was evaluated against the observed *Sphagnum* GPP and annual NPP,

710 aboveground tree biomass and shrub stem biomass. The new model can capture the

711 seasonal dynamics of moss *Sphagnum* GPP, but with lower peak GPP compared to site-

712 level observations, and can predict reasonable annual values for *Sphagnum* NPP but with

713 lower interannual variation. Our model largely agrees with observed tree and shrub

714 biomass. The model predicts that different PFTs responded differently to warming levels

715 under both ambient and elevated CO_2 concentration conditions. The NPP of the two

716 dominant tree PFTs (black spruce and *Larix*) showed contrasting responses to warming

717 scenarios (increasing with warming for *Larix* but decreasing for black spruce), while

718 shrub NPP had similar warming response to *Larix*. Hummock and hollow *Sphagnum*

719 showed opposite warming responses: hollow *Sphagnum* shows generally higher growth

720 with warming, but the hummock *Sphagnum* demonstrates more variability and strong

721 dependence with water table height. The ELM predictions further suggest that the effects

722 of CO_2 fertilization can change the direction of the warming response for the bog

723 peatland ecosystem, though observations of *Sphagnum* species at the site does not yet

724 appear to support this (Norby et al. 2019).

725 Data availability. The model code we used is available here:
726 https://github.com/dmricciuto/CLM_SPRUCE. The datasets and scripts were used for the figures
727 is here: https://github.com/dmricciuto/CLM_SPRUCE/tree/master/analysis/Shietal2020
728
729

Biogeosciences
Discussions
EGU
Open Access

736 **References:**

737 Ackermann, K., Zackrisson, O., Rousk, J., Jones, D. L., and DeLuca, T. H.: N2 fixation
738   in feather mosses is a sensitive indicator of N deposition in boreal forests, Ecosystems,
739   15, 986-998, 2012.

740 Barber, V. A., Juday, G. P., and Finney, B. P..: Reduced growth of Alaskan white spruce
741   in the twentieth century from temperature-induced drought stress, Nature, 405,668-
742   673, 2000.

743

744 Berg, A., Danielsson, A., and Sevensson, B.H.: Transfer of fixed-N from N2-fixing
745   cyanobacteria associated with moss sphagnum riparium results in enhanced growth of
746   the moss, plant and soil, 362, 271-278, https://doi.org/10.1007/s11104-012-1278-4,
747   2013.
748 Belyea, L. R. and Baird, A. J.: Beyond "The limits to peat bog growth": Cross-scale
749   feedback in peatland development, Ecol. Monogr., 76, 299-322, 2006.
750 Blok, D., Heijmans, M., Schaepman-Strub, G., Van Ruijven, J., Parmentier, F.,
751   Maximov, T., and Berendse, F.: The cooling capacity of mosses: Controls on water
752   and energy fluxes in a Siberian tundra site, Ecosystems, 14, 1055-1065, 2011.
753 Bond-Lamberty, B., Peckham, S. D., Ahl, D. E., and Gower, S. T.: Fire as the dominant
754   driver of central Canadian boreal forest carbon balance, Nature, 450, 89-92, 2007.

755 Bragazza, L., Buttler, A., Robroek, B. J., Albrecht, R., Zaccone, C., Jassey, V. E., and
756   Signarbieux, C.: Persistent high temperature and low precipitation reduce peat carbon
757   accumulation, Global Change Biology, 22, 4114-4123,
758   https://doi.org/10.1111/gcb.13319, 2016.

759 Breeuwer, A., Heijmans, M. M., Robroek, B. J., and Berendse, F.: The effect of
760   temperature on growth and competition between Sphagnum
761   species, Oecologia,156(1),155-167, doi:10.1007/s00442-008-0963-8, 2008.

762 Brown, S. M., Petrone, R. M., Mendoza, C., and Devito, K. J.: Surface vegetation
763   controls on evapotranspiration from a sub-humid Western Boreal Plain wetland,
764   Hydrological Processes, 24(8), 1072-1085, 2010.

765   Busby, J.R., Bliss, L.C., and Hamilton, C.D.: Microclimate control of growth rates and
766   habitats of the Boreal Forest Mosses, Tomenthypnum nitens and Hylocomium
767   splenden, Ecol Monogr, 48, 95-110, 1978.

768   Burrows, S.M., Maltrud, M.E., Yang, X., Zhu, Q., Jeffery, N., Shi., X., Ricciuto, D.M.,
769   Wang, S., Bisht, G., Tang, J., Wolfe, J. D., Harrop, B. E., Singh, B., Brent, L., Zhou,
770   Tian, Cameron-Smith P. J., Keen, N., Collier, N., Xu, M., Hunke, E.C., Elliott, S.M.,
771   Turner, A.K., Li, H., Wang, H., Golaz, J.-C., Bond-Lamberty, B., Hoffman, F.M.,
772   Riley, W.J., Thornton, P.E., Calvin, K., and Leung, L.R.: The DOE E3SM coupled
773   model v1.1 biogeochemistry configuration: overview and evaluation of coupled
774   carbon-climate experiments, J. Adv. Model Earth Sy., in review, 2019.
775   Gorham, E.: Northern peatlands: role in the carbon cycle and probable responses to
776   climatic warming, Ecological Applications, 1, 182-195, 1991.

777   Camill, P. and Clark, J. S.: Long-term perspectives on lagged ecosystem responses to
778   climate change: permafrost in boreal peatlands and the grassland/woodland boundary,
779   Ecosystems, 3, 534–544, 2000.

780   Chapin, F. S. III, Shaver, G.R., Giblin, A.E., Nadelhoffer, K.J., and Laundre, J.A.:
781   Responses of Arctic tundra to experimental and observed changes in climate, Ecology,
782   76, 694-711, 1995.

783   Carrell, A.A., Kolton, M., Warren, M.J., Kostka, J.E., and Weston, D. J.: Experimental
784   warming alters the community composition, diversity, and N2 fixation activity of peat
785   moss (Sphagnum fallax) microbiomes, Glob. Change Biol., 25, 2993-3004,
786   dio:10.1111/gcb.14715, 2019.

787   Chavardes, R. D., L. D. Daniels, P. O. Waeber, J. L.Innes, and C. R. Nitschke.: Unstable
788   climate-growth relations for white spruce in southwest Yukon, Canada, Climatic
789   Change, 116, 593-611, 2013.
790   Chen, W. J., Black, T. A., Yang, P.C. Barr, A.G. Neumann, H. H., Nešić, Z., Blanken, P.
791   D. Novak, M. D., Eley, J., Ketler, R., and Cuenca, R. H.:Effects of climatic variability
792   on the annual carbon sequestration by a boreal aspen forest, Glob. Change Biol., 5, 41-
793   53, 1999.
794   Clymo, R. S. and Hayward, P.M.: The ecology of Sphagnum, in: Bryophyte Ecology,
795   edited by: Smith, A. I. E., Chapman and Hall Ltd., London, New York, 229-289, 1982.

796   Collatz, G.J., Ball, J.T., Grivet, C. and Berry, J.A.: Physiological and environmental-
797   regulation of stomatal conductance, photosynthesis and transpiration - a model that
798   includes a laminar boundary-layer, Agricultural and Forest Meteorology, 54, 107-
799   136,1991.

800   Collatz, G.J., Ribas-Carbo, M. and Berry, J.A.: Coupled photosynthesis- stomatal model
801   for leaves of C4 plants, Australian Journal of Plant Physiology, 19, 519-538, 1992.

802   Cornelissen, H.C., Lang, S.I., Soudzilovskaia, N.A., and During, H.J.: Comparative
803   cryptogam ecology: a review of bryophyte and lichen traits that drive
804   biogeochemistry, Annals of Botany, 99, 987–1001, 2007.

805   Davidson, E. A. and Janssens, I. A.: Temperature sensitivity of soil carbon decomposition
806   and feedbacks to climate change, Nature, 440, 165-173, 2006.

807   Dimitrov, D. D., Grant, R. F., LaFleur, P. M., and Humphreys, E.: Modelling the effects
808   of hydrology on gross primary productivity and net ecosystem productivity at Mer
809   Bleue bog, J. Geophys. Res.-Biogeo, 116, G04010, doi:10.1029/2010JG001586, 2011.

810   Dise, N. B.: Peatland response to global change, Science, 326, 810- 811,
811   https://doi.org/10.1126/science.1174268, 2009.

812   Dorrepaal, E., Toet, S., van Logtestijn, R. S. P., Swart, E., van de Weg, M. J., Callaghan,
813   T. V., and Aerts, R.: Carbon respiration from subsurface peat accelerated by climate
814   warming in the sub- arctic, Nature, 460, 616-619, 2009.

815   Duarte, H. F., Raczka, B. M., Ricciuto, D. M., Lin, J. C., Koven, C. D., Thornton, P. E.,
816   Bowling, D. R., Lai, C. T., Bible, K. J. and Ehleringer, J. R.: Evaluating the
817   Community Land Model (CLM4.5) at a coniferous forest site in northwestern United
818   States using flux and carbon-isotope measurements, Biogeosciences, 14(18): 4315-
819   4340, DOI: 10.5194/bg-14-4315-2017, 2017.
820   Euskirchen, E.S., McGuire, A.D., Chapin, F.S. III, Yi, S., and Thompson, C.C.: Changes
821   in vegetation in northern Alaska under scenarios of climate change, 2003–2100:
822   implications for climate feedbacks, Ecological Applications 19: 1022-1043, 2009.

823   Farquhar, G.D., von Caemmerer, S. and Berry, J.A.: A biochemical model of
824   photosynthetic CO2 assimilation in leaves of C3 species. Planta, 149, 78-90, 1980.

825   Frolking, S. and Roulet, N.T.: Holocene radiative forcing impact of northern peatland
826   carbon accumulation and methane emissions, Glob. Change Biol. 13, 1079-1088,
827   2007.

828
829   Frolking, S., Roulet, N. T., Tuittila, E., Bubier, J. L., Quillet, A., Tal- bot, J., and Richard,
830   P. J. H.: A new model of Holocene peatland net primary production, decomposition,
831   water balance, and peat accumulation, Earth Syst. Dynam., 1, 1-21, doi:10.5194/esd-1-
832   1-2010, 2010.

833   Frolking, S., Talbot, J., Jones, M. C., Treat, C. C., Kauffman, Tuittila E.-S., and Roulet,
834   N.: Peatlands in the Earth's 21st century coupled climate-carbon system, Environ.
835   Rev.,19, 371-396, 2011.
836   Girardin, M. P., Bouriaud, O., Hogg, E. H., Kurz, W., Zimmermann, N. E., Metsaranta, J.
837   M., Jong, Rogier de, Frank, D. C., Esper, J., Büntgen, U., Guo, X., and Bhatti, J.: No
838   growth stimulation of Canada's boreal forest under half-century of combined warming

839   and CO_2 fertilization, Proceedings of the National Academy of Science, 113(52),
840   E8406–E8414, 2016.

841   Goetz, J.D., and Price, J.S.: Role of morphological structure and layering of Sphagnum
842   and Tomenthypnum mosses on moss productivity and evaporation rates, Canadian
843   Journal of Soil Sciences. DOI:10.4141/ CJSS-2014-092, 2015.

844   Golaz, J.-C., Caldwell, P. M.,Van Roekel, L. P., Petersen, M. R.,Tang, Q., Wolfe, J. D.,
845   Abeshu, G., Anantharaj, V., Asay-Davis, X. S., Bader, D.C., Baldwin, S. A., Bisht, G.,
846   Bogenschutz, P. A., Branstetter, M., Brunke, M., A., Brus, S.R., Burrows, S.M.,
847   Cameron-Smith P. J., Donahue, A. S., Deakin, M., Easter, R. C., Evans, K. J., Feng,
848   Y., Flanner, M., Foucar, J., G., Fyke, J. G., Griffin, B. M., Hannay, C., Harrop, B. E.,
849   Hoffman, M. J., Hunke, E. C., Jacob, R. L., Jacobsen, D. W., Jeffery, N., Jones, P. W.,
850   Klein, S. A., Larson, V. E., Leung, L. R., Li, H., Lin, W., Lipscomb, W.H., Ma, P.-L.,
851   Mahajan, S., Maltrud, M., E., Mametjanov, A., McClean, J. L., McCoy, R. B., Neale,
852   R.B., Price, S. F., Qian, Y., Rasch, P. J., Reeves Eyre, J.E.J., Riley, W. J., Ringler, T.
853   D., Roberts, A. F., Roesler, E. L., Salinger, A. G., Shaheen, Z., Shi, X., Singh, B.,
854   Tang, J., Taylor, M. A., Thornton, P. E., Tuner, A. K., Veneziani, M., Wan, H., Wang,
855   H., Wang, S., Williams, D. N., Wolfram, P. J., Worley, P. H., Xie, S., Yang, Y., Yoon,
856   J.-H., Zelinka, M. D., Zender, C. S., Zeng, X., Zhang, C., Zhang, K., Zhang, Y.,
857   Zheng, X., Zhou, T., Zhu, Q.: The DOE E3SM coupled model version 1: Overview
858   and evaluation at standard resolution, J. Adv. Model Earth Sy, 11(7), 2089-2129,
859   https://doi.org/10.1029/2018MS001603, 2019.
860   Gong, J., Roulet, N., Frolking, S., Peltola, H., Laine, A.M., Kokkonen, N., and Tuittila,
861   E.-S.: Modelling the habitat preference of two key sphagnum species in a poor fen as
862   controlled by capitulum water retention, Biogeosciences Discussions,
863   https://dio.org/10.5194/bg-2019-366, 2019.
864   Gorham, E.: Northern peatlands: role in the carbon cycle and probable responses to
865   climatic warming, Ecological Applications, 1, 182-195, 1991.

866   Grant, R. F., Desai, A. R., and Sulman, B. N.: Modelling contrasting responses of
867   wetland productivity to changes in water table depth, Biogeosciences, 9, 4215-4231,
868   2012.

869   Granath, G., Limpens, J., Posch, M., Mücher, S., and De Vries, W.: Spatio-temporal
870   trends of nitrogen deposition and climate effects on Sphagnum productivity in
871   European peatlands, Environmental Pollution, 187, 73-80, https://doi.org/10.1016/j.
872   envpol.2013.12.023, 2014Griffiths, N. A., and Sebestyen, S. D.: Dynamic vertical
873   profiles of peat porewater chemistry in a northern peatland, Wetlands, 36(6), 1119-
874   1130, 2016.

875   Griffiths, N. A., and Sebestyen, S. D.: Dynamic vertical profiles of peat porewater
876   chemistry in a northern peatland, Wetland, 36, 1119-1130, doi:10.1007/s13157-016-
877   0829-5, 2016.
878   Griffiths, N. A., Hanson, P. J., Ricciuto, Iversen, C. M., Jensen, A.M., Malhotra, A.,
879   McFarlane, K. J., Norby, R. J., Sargsyan, K., Sebestyen, S. D., Shi, X., Walker, A. P.,
880   Ward, E. J., Warren, J. M., and Weston, D, J.:Temporal and spatial variation in

881   peatland carbon cycling and implications for interpreting responses of an ecosystem-
882   scale warming experiment, Soil Sci. Soc. Am. J., 81(6), 1668-1688,
883   doi:10.2136/sssaj2016.12.0422, 2018.
884   Gundale, M.J., DeLuca, T.H., and Nordin, A.: Bryophytes attenuate anthropogenic
885   nitrogen inputs in boreal forests, Glob. Change Biol.,17, 2743-2753, 2011.

886   Hanson, P. J., Riggs, J.S., Nettles, W. R., Krassovski, M. B., and Hook L. A.: SPRUCE
887   deep peat heating (DPH) environmental data, February 2014 through July 2015, Oak
888   Ridge National Laboratory, TES SFA, U.S. Department of Energy, Oak Ridge,
889   Tennessee, U.S.A. https://doi.org/10.3334/CDIAC/spruce.013, 2015a.
890   Hanson, P.J., Riggs, J.S. Dorrance, C., Nettles, W.R., and Hook, L.A.: SPRUCE
891   Environmental Monitoring Data: 2010-2016. Carbon Dioxide Information Analysis
892   Center, Oak Ridge National Laboratory, U.S. Department of Energy, Oak Ridge,
893   Tennessee, U.S.A. http://dx.doi.org/10.3334/CDIAC/spruce.001, 2015b.

894   Hanson, P. J., Gill, A. L., Xu, X., Phillips, J. R., Weston, D. J., Kolka, R. K., Riggs, J.
895   S., and Hook, L. A.: Intermediate-scale community-level flux of CO2 and CH4 in a
896   Minnesota peatland: putting the SPRUCE project in a global context,
897   Biogeochemistry, 129(3), 255-272, 2016.

898   Hanson, P. J., Riggs, J.S., Nettles, W.R., Phillips, J.R., Krassovski, M.B., Hook, L.A.,
899   Gu, L., Richardson, A.D., Aubrecht, D.M., Ricciuto, D.M., Warren, J.M., and Barbier,
900   C.: Attaining whole-ecosystem warming using air and deep-soil heating methods with
901   an elevated CO2 atmosphere, Biogeosciences, 14, 861-883, 2017.
902
903   Hanson, P.J., Phillips, J.R., Wullschelger, S. D., Nettles, W. R., Warren, J. M., Ward, E.
904   J.: SPRUCE Tree Growth Assessments of Picea and Larix in S1-Bog Plots and
905   SPRUCE Experimental Plots beginning in 2011, Oak Ridge National Laboratory, TES
906   SFA, U.S. Department of Energy, Oak Ridge, Tennessee,
907   U.S.A. https://doi.org/10.25581/spruce.051/1433836, 2018a.
908
909   Hanson, P.J., Phillips, J.R., Brice, D.J., and Hook, L.A.: SPRUCE Shrub-Layer Growth
910   Assessments in S1-Bog Plots and SPRUCE Experimental Plots beginning in
911   2010. Oak Ridge National Laboratory, TES SFA, U.S. Department of Energy, Oak
912   Ridge, Tennessee, U.S.A. https://doi.org/10.25581/spruce.052/1433837, 2018b.

913   Heijmans, M.M.P.D., Arp, W.J., and Chapin, F.S. III.: Carbon dioxide and water vapour
914   exchange from understory species in boreal forest, Agricultural and Forest
915   Meteorology 123,135-147, DOI:10.1016/j. agrformet.2003.12.006, 2004a.

916   Heijmans, M.M.P.D, Arp, W.J., and Chapin, F.S. III.: Controls on moss evaporation in a
917   boreal black spruce forest. Global Biogeochemical Cycles 18(2), 1-8,
918   DOI:10.1029/2003GB002128, 2004b.

919   Heijmans, M.M. P. D., Mauquoy, D., van Geel, B., and Berendse, F.: Long-term effects
920   of climate change on vegetation and carbon dynamics in peat bogs. Journal of
921   Vegetation Science 19, 307-320, 2008.

922 Hobbie, S.E., and Chapin, F.S. III.: The response of tundra plant biomass, aboveground
923   production, nitrogen, and CO2 flux to experimental warming, Ecology, 79,1526-1544,
924   1998.

925 Hobbie, S.E., Shevtsova, A., and Chapin, F.S.III.: Plant responses to species removal and
926   experimental warming in Alaskan Tus- sock Tundra. Oikos 84,417-434, 1999.

927 Ise, T., Dunn, A. L., Wofsy, S. C., and Moorcroft, P. R.: High sensitivity of peat
928   decomposition to climate change through water table feedback, Nat. Geosci., 1, 763-
929   766, 2008.

930 Jensen, A.M., Warren, J. M., Hook, L. A., Wullschleger, S. D., Brice, D.J., Childs, J.,
931   and Vander Stel, H.M.: SPRUCE S1 Bog Pretreatment Seasonal Photosynthesis and
932   Respiration of Trees, Shrubs, and Herbaceous Plants, 2010-2015, Oak Ridge National
933   Laboratory, TES SFA, U.S. Department of Energy, Oak Ridge, Tennessee, U.S.A.,
934   https://doi.org/10.3334/CDIAC/spruce.008, 2018.
935 Jensen, A.M., Warren, J. M., King, A., Ricciuto, D.M., Hanson, P. J., and Wullschleger,
936   S. D.:Simulated projections of boreal forest peatland ecosystem productivity are
937   sensitive to observed seasonality in leaf phenology, Tree Physiology, 39(4), 556-572,
938   doi: 10.1093/treephys/tpy140, 2019.

939
940 Jiang, J., Huang, Y., Ma, S., Stacy, M., Shi, Z., Ricciuto, D. M., Hanson, P. J., and Luo,
941   Y.: Forecasting Responses of a Northern Peatland Carbon Cycle to Elevated CO_2 and
942   a Gradient of Experimental Warming, J. Geophys. Res.-Biogeo, 123(3), 1057-1071,
943   doi: 10.1002/2017JG004040, 2018.
944 Juday, G. P., and Alix, C.: Consistent negative temperature sensitivity and positive
945   influence of precipitation on growth of floodplain Picea glaucain Interior Alaska,
946   Canadian Journal of Forest Research, 42, 561-573, 2012.
947
948
949 Kostka, J.E., Weston, D.J., Glass, J.B., Lilleskov, E.A., Shaw, A.J., and Turetsky, M.R.:
950   The Sphagnum microbiome: new insights from an ancient plant lineage, New
951   Phytologist, 211(1):57-64, 2016

952 Kuiper, J. J., Mooij, W. M., Bragazza, L., and Robroek, B. J.: Plant functional types
953   define magnitude of drought response in peatland CO_2 exchange, Ecology, 95, 123-
954   131, https://doi.org/10.1890/13-0270.1, 2014.

955 Lafleur, P. M., Hember, R. A., Admiral, S. W., and Roulet, N. T.: Annual and seasonal
956   variability in evapotranspiration and water table at a shrub-covered bog in southern
957   Ontario, Canada, Hydrol. Process., 19, 3533–3550, https://doi.org/10.1002/hyp.5842,
958   2005.

959 Launiainen, S., Katul, G. G., Lauren, A., and Kolari, P.: Coupling boreal forest CO_2, H_2O
960   and energy flow by a vertically structured forest canopy-Soil model with separate

961   bryophyte layer. Ecological Modelling, 312, 385-405.
962   https://doi.org/10.1016/j.ecolmodel.2015.06.007, 2015.

963   Limpens, J., Berendse, F., Blodau, C., Canadell, J. G., Freeman, C., Holden, J., Roulet,
964   N., Rydin, H., and Schaepman-Strub, G.:Peatlands and the carbon cycle: From local
965   processes to global implications-A synthesis, Biogeosciences, 5(5), 1475-1491,
966   doi:10.5194/bg-5-1475-2008, 2008.
967   Lindo, Z, and Gonzalez, A.: The bryosphere: an integral and influential component of the
968   earth's biosphere, Ecosystems, 13, 612–627, 2010.

969   Lindo, Z., Nilsson, M.C., and Gundale, M.J.: Bryophyte-cyanobacteria associations as
970   regulators of the northern latitude carbon balance in response to global change, Glob.
971   Change Biol., 19(7),2022-35, 2013.

972   Lu, D., Ricciuto, D.M., Stoyanov, M., and Gu, L.: Calibration of the E3SM Land Model
973   Using Surrogate-Based Global Optimization, J Adv Model Earth Sy, 10(6), 1337-
974   1356, doi: 10.1002/2017ms001134, 2018.

975   Lu, D., and Ricciuto, D.M.: Efficient surrogate modeling methods for large-scale Earth
976   system models based on machine-learning techniques, Geosci Model Dev, 12(5),
977   1791-1807, doi: 10.5194/gmd-12-1791-2019, 2019.

978   Man, R., Kayahara, G.J., Rice, J.A., and MacDonald, G.B.: Eleven- year responses of a
979   boreal mixedwood stand to partial har- vesting: light, vegetation, and regeneration
980   dynamics, For Ecol Manag 255,697-706, 2008.

981   Mazziotta, A., Granath, G., Rydin, H. and Bengtsson F.: Scaling functional traits to
982   ecosystem processes: Towards a mechanistic understanding in peat mosses, Journal of
983   Ecology, DOI:10.1111/1365-2745.13110, 2018.

984   Metcalfe, D. B., Ricciuto D. M., Palmroth, S., Campbell, Hurry, C., V., Mao, J., Keel, S.
985   G., Linder, S., Shi, X., Näsholm, T., Ohlsson, K. E. A., Blackburn, M., Thornton, P. E.
986   and Oren, R.: Informing climate models with rapid chamber measurements of forest
987   carbon uptake, Global Change Biology, 23(5), 2130-2139, DOI: 10.1111/gcb.13451,
988   2017.

989   McFadden, J.P., Eugster, W., Chapin, F.S.III.: A regional study of the controls on water
990   vapor and CO2 exchange in Arctic tundra, Ecology, 84,2762-76, 2003.

991   McGuire, A. D., Anderson, L. G., Christensen, T. R., Dallimore, S., Guo, L., Hayes, D.
992   J., Heimann, M., Lorenson, T. D., Macdonald, R. W. and Roulet, N.: Sensitivity of the
993   carbon cycle in the Arctic to climate change, Ecol. Monogr., 79, 523-555, 2009.

994   Miller, P. A. and Smith, B.: Modelling Tundra Vegetation Response to Recent Arctic
995   Warming, Ambio, 41, 281-291, https://doi.org/10.1007/s13280-012-0306-1, 2012.

996 Mokhov, I.I., Eliseev, A.V., and Denisov, S.N.: Model diagnostics of variations in
997   methane emissions by wetlands in the second half of the 20th century based on
998   reanalysis data, Dokl. Earth Sci., 417(1),1293-1297, 2007.

999   Moore, T.R., Roulet, N.T., and Waddington, J.M.: Uncertainty in predicting the effect of
1000   climate change on the carbon cycling of Canadian peatlands, Clim. Change, 40, 229-
1001   245, 1998.
1002 Myneni, R. B., Keeling, C. D., Tucker, C. J., Asrar, G., and Nemani, R. R.: Increased
1003   plant growth in the northern high latitudes from 1981 to 199,1 Nature, 386,698-702,
1004   1997.

1005 Murray, K.J., Tenhunen, J.D., and Nowak, R.S.: Photoinhibition as a control on
1006   photosynthesis and production of Sphagnum mosses, Oecologia, 96,200-207, 1993.

1007 Nichols, J.E., and Peteet, D.M.: Rapid expansion of northern peatlands and doubled
1008   estimate of carbon storage, Nat. Geosci. 12, 917-921, doi:10.1038/s41561-019-0454-z,
1009   2019.
1010 Nilsson, M.C., and Wardle, D.A.: Understory vegetation as a forest ecosystem driver:
1011   evidence from the northern Swedish boreal forest, Frontiers in Ecology and the
1012   Environment, 3, 421-428, 2005.
1013 Norby, R.J., and Childs, J.: Sphagnum productivity and community composition
1014   in the SPRUCE experimental plots. Carbon Dioxide Information Analysis
1015   Center, Oak Ridge National Laboratory, U.S. Department of Energy, Oak
1016   Ridge, Tennessee, U.S.A. http://dx.doi.org/10.3334/CDIAC/spruce.xxx, 2017.

1017 Norby, R.J., Childs, J., Hanson, P.J., and Warren, J.M..: Rapid loss of an ecosystem
1018   engineer: Sphagnum decline in an experimentally warmed bog, Ecology and
1019   Evolution, 9(22), 12571-12585, https://doi.org/10.1002/ece3.5722, 2019.
1020 Nungesser, M. K.: Modelling microtopography in boreal peatlands:Hummocks and
1021   hollows, Ecol. Model.,165(2-3), 175-207, 2003.
1022
1023 Oechel, W.C., and Van Cleve, K.: The role of bryophytes in nutrient cycling in the taiga,
1024   in Ecological Studies, Vol. 57: Forest Ecosystems in the Alaskan Taiga, edited by:
1025   Van Cleve, K., Chapin III, F. S., Flanagan, P.W., Viereck, L.A., and Dyrness, C.T.,
1026   Springer-Verlag, New York, 121-137,1986.

1027 Oleson, K. W., Lawrence, D. W., Bonan, G. B., Drewniak, B., Huang, M., Koven, C. D.,
1028   Levis, S., Li, F., Riley, W. J., Subin, Z. M., Swenson, S. C., Thornton, P. E., Bozbiyik,
1029   A., Fisher, R., Heald, C. L., Kluzek, E., Lamarque, J., Lawrence, P. J., Leung, L. R.,
1030   Lipscomb, W., Muszala, S., Ricciuto, D. M., Sacks, W., Sun,Y., Tang, J., and Yang,
1031   Z.: Technical description of version 4.5 of the Community Land Model (CLM),
1032   NCAR/TN-503+STR, NCAR Technical Note, 2013.

1033 Park, H., Launiainen, S., Konstantinov, P. Y., Iijima, Y., and Fedorov, A. N.: Modeling
1034   the effect of moss cover on soil temperature and carbon fluxes at a tundra site in
1035   northeastern Siberia, J. Geophys. Res.-Bioge, 123, 3028-3044, https://doi.org/
1036   10.1029/2018JG004491, 2018.

1037   Parsekian, A. D., Slater, L., Ntarlagiannis, D., Nolan, J., S. Sebestyen, D., Kolka, R. K.,
1038   and Hanson, P. J.: Uncertainty in peat volume and soil carbon estimated using ground-
1039   penetrating radar and probing. Soil Sci. Soc. Am. J., 76, 1911-1918. DOI:
1040   10.2136/sssaj2012.0040, 2012.
1041   Pastor, J., Peckham, B., Bridgham, S., Weltzin, J., and Chen, J.: Plant community
1042   dynamics, nutrient cycling, and alternative stable equilibria in peatlands, The
1043   American Naturalist 160, 553-568, 2002.

1044   Peichl, M., Öquist, M., Löfvenius, M. O., Ilstedt, U., Sagerfors, J., Grelle, A., Lindroth,
1045   A., and Nilsson, M. B.: A 12-year record reveals pre-growing season temperature and
1046   water table level threshold effects on the net carbon dioxide exchange in a boreal fen,
1047   Environ. Res. Lett., 9, 055006, https://doi.org/10.1088/1748- 9326/9/5/055006, 2014.

1048   Petrone, R., Solondz, D., Macrae, M., Gignac, D., and Devito, K.J.: Microtopographical
1049   and canopy cover controls on moss carbon dioxide exchange in a western boreal plain
1050   peatland, Ecohydrology, 4, 115-129, 2011.

1051   Raczka, B., Duarte, H. F., Koven, C. D., Ricciuto, D.M., Thornton, P. E., Lin, J. C. and
1052   Bowling, D. R.: An observational constraint on stomatal function in forests: evaluating
1053   coupled carbon and water vapor exchange with carbon isotopes in the Community
1054   Land Model (CLM4.5), Biogeosciences, 13(18), 5183-5204, DOI: 10.5194/bg-13-
1055   5183-2016, 2016.
1056   Raghoebarsing, A. A., Smolders, A.J.P., Schmid, M.C., Rijpstra, W.I.C., Wolters-Arts,
1057   M., Derksen, J., Jetten, M.S.M., Schouten, S., Sinninghe Damsté, J.S., Lamers,
1058   L.P.M., Roelofs, J.G.M., Op den Camp, H.J.M., and Strous, M.: Methanotrophic
1059   symbionts provide carbon for photosynthesis in peat bogs. Nature, 436, 1153-1156,
1060   doi:10.1038/nature03802, 2005.
1061
1062   Ricciuto, D. M., Sargsyan, K., and Thornton, P.E.: The Impact of Parametric
1063   Uncertainties on Biogeochemistry in the E3SM Land Model, J Adv Model Earth Sy,
1064   10(2), 297-319, doi: 10.1002/2017ms000962, 2018.

1065   Ricciuto, D.M., Xu, X., Shi, X., Wang, Y., Song, X., Schadt, C.W., Griffiths, N. A., Mao,
1066   J., Warre, J.,M., Thornton, P.E., Chanton, J., Keller, J., Bridgham, S., Gutknecht, J.,
1067   Sebestyen, S. D., Finzi, A., Kolka, R., and Hanson P.J.: An Integrative Model for Soil
1068   Biogeochemistry and Methane Processes: I. Model Structure and Sensitivity Analysis,
1069   J. Geophys. Res.-Biogeo, In review, 2019.

1070   Riutta, T., Laine, J., and Tuittila, E.-S.: Sensitivity of CO2 exchange of fen ecosystem
1071   componetns to water level variation, Ecosystem, 10(5), 718-733, 2007.

1072   Robroek, B.J.M., Limpens, J., Breeuwer, A., and Schouten, M.G.C.: Effects of water
1073   level and temperature on performance of four Sphagnum mosses. Plant
1074   Ecology, 190, 97-107, 2007.
1075   Robroek, B.J.M., Schouten, M.G.C., Limpens, J., Berendse F. and Poorter, H.: Interactive
1076   effects of water table and precipitation on net CO2 assimilation of three co-occurring
1077   Sphagnum mosses differing in distribution above the water table, Glob. Change Biol.,

1078   15, 680-691, 2009.

1079 Rosenzweig, C., Karoly, D., Vicarelli, M., Neofotis, P., Wu, Q., Casassa, G., Menzel, A.,
1080   Root, T., Estrella, N., Seguin, B., Tryjanowski, P., Liu, C., Ravlins, S., and Imeson,
1081   A.: Attributing physical and biological impacts to anthropogenic climate
1082   change, Nature, 453, 353-357, doi:10.1038/nature06937, 2008.
1083 Rydin, H., and Jeglum, J.: The Biology of Peatlands, 343 pp., Oxford University Press,
1084   New York, 2006.
1085 Rousk, K., Rousk, J., Jones, D.L., Zackrisson, O., DeLuca, and T.H..: Feather moss
1086   nitrogen acquisition across natural fertility gradients in boreal forests, Soil Biol
1087   Biochem, 61, 86-95, 2013.

1088 Rousk, K., and Michelsen, A.: The sensitivity of Moss-Associated Nitrogen Fixtion
1089   towards Repeated Nitrogen Input, Plos One, 11(1), e0146655,
1090   https://doi.org/10.1371/journal.pone.0146655, 2016.

1091 Rydsaa, J. H., Stordal, F., Bryn, A., and Tallaksen, L. M.: Effects of shrub and tree cover
1092   increase on the near-surface atmosphere in northern Fennoscandia, Biogeosciences,
1093   14, 4209-4227, https://doi.org/10.5194/bg-14-4209-2017, 2017.
1094
1095 Sargsyan, K., Safta, C., Najm, H. N., Debusschere, B. J., Ricciuto, D.M., and Thornton,
1096   P.E.: Dimensionality Reduction for Complex Models Via Bayesian Compressive
1097   Sensing, International Journal for Uncertainty Quantification, 4(1), 63-93, doi:
1098   10.1615/Int.J.UncertaintyQuantification.2013006821, 2014.
1099 Sebestyen, S. D., Dorrance, C., Olson, D. M., Verry, E. S., Kolka, R. K., Elling, A. E.,
1100   and Kyllander, R.: Long-term monitoring sites and trends at the Marcell Experimental
1101   Forest, in: Peatland biogeochemistry and watershed hydrology at the Marcell
1102   Experimental Forest, edited by: Kolka, R. K. Sebestyen, S. D., Verry, E. S., and
1103   Brooks, CRC Press, New YorK, 15-71, 2011.

1104 Shi, X., Thornton, P. E., Ricciuto, D. M., Hanson, P. J., Mao, J., Sebestyen, S. D.,
1105   Griffiths, N. A., and Bisht, G.: Representing northern peatland microtopography and
1106   hydrology within the Community Land Model, Biogeosciences, 12(21), 6463-6477,
1107   https://doi.org/10.5194/bg-12-6463-2015, 2015.
1108 Silva, L. C. R., Anand, M., and Leithead, M. D.: Recent widespread tree growth decline
1109   despite increasing atmospheric CO2, PLoS ONE, 5(7), e11543, doi:
1110   10.1371/journal.pone.0011543, 2010.
1111
1112 Sonnentag, O., Van Der Kamp, G., Barr, A.G., and Chen, J.: on the relationship between
1113   water table depth and water vapor and carbon dioxide fluxes in a minerotrophic fen,
1114   Glob. Change Biol., 16(6), 1761-1776, https://doi.org/10.1111/j.1365-
1115   2486.2009.02032.x, 2010.
1116 St-Hilaire, F., Wu, J., Roulet, N. T., Frolking, S., Lafleur, P. M., Humphreys, E. R., and
1117   Arora, V.: McGill wetland model: evalu- ation of a peatland carbon simulator
1118   developed for global assessments, Biogeosciences, 7, 3517-3530, 2010.

1119 Sulman, B. N., Desai, A. R., Saliendra, N. Z., Lafleur, P. M., Flana- gan, L. B.,
1120   Sonnentag, O., Mackay, D. S., Barr, A. G., and Kamp, G. V. D.: CO2 fluxes at
1121   northern fens and bogs have opposite responses to inter-annual fluctuations in water
1122   table,Geophys.Res. Lett., 37, L19702, doi:10.1029/2010GL044018, 2010.

1123 Tarnocai, C.: The effect of climate change on carbon in Canadian peatlands, Glob Planet
1124   Change, 53, 4, 222-232, 2006.
1125 Tenhunen, J.D., Weber, J.A., Yocum, C.S. and Gates, D.M.: Development of a
1126   photosynthesis model with an emphasis on ecological applications, Oecologia, 26,101-
1127   119, 1976.

1129 Tian, H., Lu,C., Yang, J., Banger, K., Huntinzger, D. N., Schwalm, C. R., Michalak, A.
1130   M., Cook, R., Ciais, P., Hayes, D., Huang, M., Ito, A., Jacobson, A., Jain,A., Lei, H.,
1131   Mao,J., Pan, S., Post, W.M, Peng, S., Poulter,B., Ren, W., Ricciuto,D.M., Schaefer, K.,
1132   Shi, X., Tao,B., Wang, W., Wei, Y., Yang, Q., Zhang, B., and Zeng, N.: Global patterns
1133   of soil carbon stocks and fluxes as simulated by multiple terrestrial biosphere models:
1134   sources and magnitude uncertainty, Global Biogeochem Cycles, 29, 775-792.
1135   doi:10.1002/2014GB005021, 2015.
1136 Titus, J. E., Wagner, D.J., and Stephens, M.D.: Contrasting Water Relations of
1137   Photosynthesis for 2 Sphagnum Mosses, Ecology, 64, 1109-1115, 1983.

1138 Todd-Brown, K. E. O., Randerson, J. T., Post, W. M., Hoffman, F. M., Tarnocai, C.,
1139   Schuur, E. A. G., and Allison, S. D.: Causes of variation in soil carbon simulations
1140   from CMIP5 Earth system models and comparison with observations, Biogeosciences,
1141   10, 1717–1736, doi:10.5194/bg-10-1717-2013, 2013.

1142 Turetsky, M. R., Wieder, R. K., and Vitt, D. H.: Boreal peatland C fluxes under varying
1143   permafrost regimes, Soil Biol. Biochem.,34,907-912, 2002.
1144 Turetsky, M.R., Mack, M.C., Hollingsworth, T.N., and Harden, J.W.: The role of mosses
1145   in ecosystem succession and function in Alaska's boreal forest, Canadian Journal of
1146   Forest Research 4, 1237-1264, 2010.
1147 Turetsky, M. R., Bond-Lamberty, B., Euskirchen, E., Talbot, J., Frolking, S., McGuire,
1148   A. D., and Tuittila, E.-S.: The resilience and functional role of moss in boreal and arc-
1149   tic ecosystems, New Phytol., 196, 49-67, doi:10.1111/j.1469- 8137.2012.04254.x,
1150   2012.

1152 Van, B. N.: How Sphagnum bogs down other plants, Trends Ecol. Evol, 10, 270-275,
1153   1995.

1155 van der Schaaf, S.: Bog hydrology, in: Conservation and Restoration of Raised Bogs:
1156   Geological, Hydrological and Ecological Studies, edited by: Schouten, M.G.C., The
1157   Government Stationery Office, Dublin, 54-109, 2002.

1158 van der Wal, R., Pearce, I.S.K and Brooker, R.W.: Mosses and the struggle for light in a
1159   nitrogen-polluted world, Oecologia, 142,159-68, 2005.

1160 Verry, E. S., and Jansenns, J.: Geology, vegetation, and hydrology of the S2 bog at the
1161   MEF: 12,000 years in northern Minnesota, in Peatland biogeochemistry and watershed
1162   hydrology at the Marcell Experimental Forest, edited by R. K. Kolka   S. D.
1163   Sebestyen, E. S. Verry, K.N. Brooks, CRC Press, New YorK, 93-134, 2011.
1164

1165 Vile, M. A., Kelman Wieder, R., Živković, T., Scott, K. D., Vitt, D. H., Hartsock, J. A.,
1166   Iosue, C. L., Quinn, J.C., Petix, M., Fillingim, H.M., Popma, J.M.A., Dynarski, K.A.,
1167   Jackman, T. R., Albright, C.M., and Wykoff, D. D. : N2-fixation by methanotrophs
1168   sustains carbon and nitrogen accumulation in pristine peatlands, Biogeochemistry,
1169   121, 317-328, https://doi.org/10.1007/ s10533-014-0019-6, 2014.

1170 Vitt, D. H.: A key and review of bryophytes common in North American peatlands,
1171   Evansia, 31, 121-158, 2014.

1172 Wania, R., Ross, I., Prentice, I.C.: Integrating peatlands and permafrost into a dynamic
1173   global vegetation model: 1. Evaluation and sensitivity of physical land surface
1174   processes, Global Biogeochem. Cycles 23, GB3014, doi:10.1029/2008GB003412,
1175   2009.

1176 Wania, R., Melton, J. R., Hodson, E. L., Poulter, B., Ringeval, B., Spahni, R., Bohn, T.,
1177   Avis, C. A., Chen ,G., Eliseev, A. V., Hopcroft, P. O., Riley, W. J., Subin, Z. M., Tian,
1178   H., van Bodegom, P.M. , Kleinen, T. , Yu, Z., Singarayer, J. S., Zurcher, S.,
1179   Lettenmaier, D. P., Beerling, D. J., Denisov, S. N., Prigent, C., Papa, F., and Kaplan, J.
1180   O.: Present state of global wetland extent and wetland methane modelling:
1181   methodology of a model inter-comparison project (WETCHIMP), Geosci. Model
1182   Dev., 6, 617-641, 2013.

1183 Walker, M.D., Wahren, C.H., Hollister, R.D., Henry, G.H.R., Ahlquist, L.E., Alatalo,
1184   J.M., Bret-Harte, M.S., Calef, M.P., Callaghan, T.V., Carroll, A.B., Epstein, H.E.,
1185   Jonsdottir, I.S., Klein, J.A., Magnusson, B., Molau, U., Oberbauer ,S.F., Rewa, S.P.,
1186   Robinson, C.H., Shaver, G.R., Suding, K.N., Thompson, C.C., Tolvanen, A., Totland,
1187   O., Turner, P.L., Tweedie, C.E., Webber, and P.J., Wookey, P.A.: Plant community
1188   responses to experimental warming across the tundra biome, Proc Natl Acad Sci USA,
1189   10,31342-6, 2006.

1190 Walker, T. N., Ward, S. E., Ostle, N. J., and Bardgett, R. D.: Contrasting growth
1191   responses of dominant peatland plants to warming and vegetation composition,
1192   Oecologia, 178, 141-151, https://doi. org/10.1007/s00442-015-3254-1, 2015.

1193 Walker, A. P., Carter, K. R., Gu, L., Hanson, P. J., Malhotra, A., Norby, R.J., Sebestyen,
1194   S. D., Wullschleger, S. D., Weston, D. J.: 2017. Biophysical drivers of seasonal
1195   variability in Sphagnum gross primary production in a northern temperate bog, J.
1196   Geophys. Res.-Biogeo, 122, 1078-1097, https://doi.org/10.1002/2016JG003711, 2017.

1197   Wang, H., Richardson, C. J., and Ho, M.: Dual controls on carbon loss during drought in
1198   peatlands, Nature Climate Change, 5, 58- 587, 2015.

1199   Ward, S. E., Ostle, N. J., Oakley, S., Quirk, H., Henrys, P. A., and Bardgett, R. D.:
1200   Warming effects on greenhouse gas fluxes in peatlands are modulated by vegetation
1201   composition, Ecol. Lett., 16, 1285-1293, 2013.

1202   Weston, D.J., Timm, C.M., Walker, A.P., Gu, L., Muchero, W., Schmuta, J., Shaw, A. J.,
1203   Tuskan, G. A., Warren, J.M., and Wllschleger, S.D.: Sphagnum physiology in the
1204   context of changing climate: Emergent influences of genomics, modeling and host-
1205   microbiome interactions on understanding ecosystem function, Plant, Cell and
1206   Environment, 38, 1737-1751, doi: 10.1111/pce.12458, 2015.

1207   White, M. A., Thornton, P. E., Running, S. W., and Nemani, R. R.: Parameterization and
1208   sensitivity analysis of the BIOME-BGC terrestrial ecosystem model: Net primary
1209   production controls, Earth Interactions, 4(3), 1-85, 2000.

1210   Wieder R. K.: Primary production in boreal peatlands. In: Boreal peatland ecosystems,
1211   edited by: Wieder, R. K., and Vitt, D. H., Springer-Verlag, Berlin Heidelberg,
1212   Germany, 145-163, 2006.

1213   Wiley, E., Rogers, B. J., Griesbauer, H. P., and Landhausser, S. M.: Spruce shows greater
1214   sensitivity to recent warming than Douglas-fir in central British Columbia, Ecosphere
1215   9(5), e02221, 10.1002/ecs2.2221, 2018Williams T.G. and Flanagan, L.B.: Measuring
1216   and modelling environmental influences on photosynthetic gas exchange in Sphagnum
1217   and Pleurozium, Plant Cell and Environment, 21, 555-564, 1998.

1218   Wilmking, M., Juday, G. P., Barber, V. A., and Zald, H. S. J.: Recent climate warming
1219   forces contrasting growth responses of white spruce at treeline in Alaska through
1220   temperature thresholds, Glob. Change Biol. 10,1724-1736, 2004.

1221   Wolf, A., Callaghan, T. V., and Larson, K.: Future changes in vegetation and ecosystem
1222   function of the Barents Region, Climatic Change, 87, 51-73,
1223   https://doi.org/10.1007/s10584-007-9342-4, 2008.

1224   Wolken, J. M., Mann, D. H., Grant, T. A., Lloyd, A. H., Rupp, T.S., and Hollingsworth,
1225   T. N.: 2016. Climate-growth relationships along a black spruce topose-quence in
1226   interior Alaska, Arctic, Antarctic, and Alpine Research, 48,637-652, 2016.
1227
1228   Wu, J., Roulet, N. T., Sagerfors, J., Nilsson, M. B.: Simulation of six years of carbon
1229   fluxes for a sedge-dominated oligotrophic minerogenic peatland in Northern Sweden
1230   using the McGill Wetland Model (MWM), J. Geophys. Res. -Biogeosciences,
1231   dio:10.1002/jgrg.20045, 2013.

1232   Wu, Y. and Blodau, C.: PEATBOG: a biogeochemical model for analyzing coupled
1233   carbon and nitrogen dynamics in northern peatlands, Geosci. Model Dev., 6, 1173-
1234   1207, doi:10.5194/gmd-6- 1173-2013, 2013.

1235 Wu, J. and Roulet, N. T.: Climate change reduces the capacity of northern peatlands to
1236   absorb the atmospheric carbon dioxide: The different responses of bogs and fens,
1237   Global Biogeochem. Cycles, doi.org/10.1002/2014GB004845, 2014.

1238 Wu, Y., Verseghy, D. L., and Melton, J. R.: Integrating peatlands into the coupled
1239   Canadian Land Surface Scheme (CLASS) v3.6 and the Canadian Terrestrial
1240   Ecosystem Model (CTEM) v2.0, Geosci. Model Dev., 9, 2639-2663,
1241   doi:10.5194/gmd-9-2639-2016, 2016.

1242 Yang, X., Ricciuto, D. M., Thornton, P. E., Shi, X., Xu, M., Hoffman, F., Norby R. J.:
1243   The effects of phosphorus cycle dynamics on carbon sources and sinks in the Amazon
1244   region: a modeling study using ELM v1, J. Geophys. Res.-Biogeo, 124,
1245   https://doi.org/10.1029/2019JG005082, 2019.

1246 Yu, Z., Loisel, J., Brosseau, D. P., Beilman, D. W., and Hunt, S.J.: Global peatland
1247   dynamics since the Last Glacial Maximum, Geophys. Res. Lett., 37, L13402,
1248   doi:10.1029/2010GL043584, 2010.

1249 Yurova, A., Wolf, A., Sagerfors, J., and Nilsson, M.: Variations in net ecosystem
1250   exchange of carbon dioxide in a boreal mire: Modeling mechanisms linked to water
1251   table position, J. Geophys. Res.-Biogeo., 112, G02025, doi:10.1029/2006JG000342,
1252   2007

1253 Zhang, W. X., Miller, P. A., Smith, B., Wania, R., Koenigk, T., and Doscher, R.: Tundra
1254   shrubification and tree-line advance amplify arctic climate warming: results from an
1255   individual- based dynamic vegetation model, Environ. Res. Lett., 8, 034023,
1256   https://doi.org/10.1088/1748-9326/8/3/034023, 2013.

1257 Zhuang, Q., Melillo, J.M., Sarofim, M.C., Kicklighter, D.W., McGuire, A.D., Felzer,
1258   B.S., Sokolov, A., Prinn, R.G., Steudler, P.A., and Hu, S.: CO_2 and CH_4 exchanges
1259   between land ecosystems and the atmosphere in northern high latitudes over the 21st
1260   century, Geophys. Res. Lett., 33, L17403, dio:10.1029/2006GL026972, 2006.
1261
1262